Report 3424
Part II

NAVAL SHIP RESEARCH AND DEVELOPMENT CENTER
Bethesda, Maryland 20034

APPLICATION OF THE METHOD OF INTEGRAL RELATIONS (MIR) TO TRANSONIC AIRFOIL PROBLEMS. PART II - INVISCID SUPERCRITICAL FLOW ABOUT LIFTING AIRFOILS WITH EMBEDDED SHOCK WAVE

by

Tsze C. Tai

AVIATION AND SURFACE EFFECTS DEPARTMENT

July 1972

Report 3424
Part II

APPLICATION OF THE METHOD OF INTEGRAL RELATIONS (MIR) TO TRANSONIC AIRFOIL PROBLEMS. PART II - INVISCID SUPERCRITICAL FLOW ABOUT LIFTING AIRFOILS WITH EMBEDDED SHOCK WAVE

The Naval Ship Research and Development Center is a U. S. Navy center for laboratory effort directed at achieving improved sea and air vehicles. It was formed in March 1967 by merging the David Taylor Model Basin at Carderock, Maryland with the Marine Engineering Laboratory at Annapolis, Maryland.

Naval Ship Research and Development Center
Bethesda, Md. 20034

MAJOR NSRDC ORGANIZATIONAL COMPONENTS

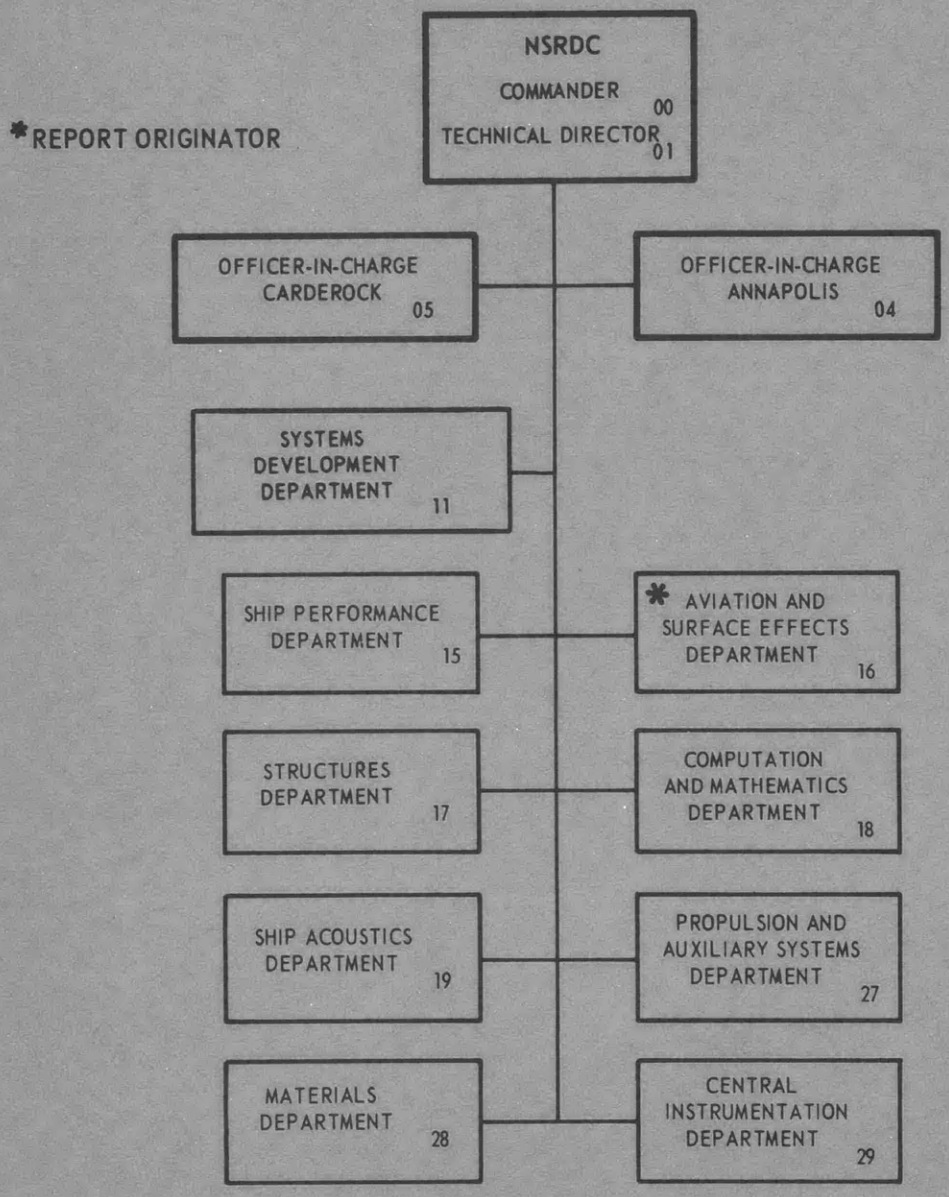

NDW-NSRDC 3960/44 (REV. 8/71)
GPO 917-872

DEPARTMENT OF THE NAVY
NAVAL SHIP RESEARCH AND DEVELOPMENT CENTER
Bethesda, Maryland 20034

APPLICATION OF THE METHOD OF INTEGRAL RELATIONS (MIR) TO TRANSONIC AIRFOIL PROBLEMS. PART II - INVISCID SUPERCRITICAL FLOW ABOUT LIFTING AIRFOILS WITH EMBEDDED SHOCK WAVE

by

Tsze C. Tai

July 1972

Report 3424
Part II
Aero Report 1176

TABLE OF CONTENTS

LIST OF FIGURES

NOTATION

A,B,Q	Functions in Equation (9)
a_j,b_j,c_j,d_j	Constants used in Equation (B-8)
a_k	Constants used in Equation (10)
C	$C \equiv 1 + 2/[(\gamma-1)M_\infty^2]$
C_r	Correction coefficient
c	Chord length of an airfoil
c_v	Specific heat at constant volume
$D/D\xi$	Derivative along a streamline
E	Function defined by Equations (A-10)
I	An integral
K	$K \equiv 1/(\gamma M_\infty^2)$
k	Constant evaluated by Equation (18b)
L	Lagrange multiplier function as given by Equation (12b)
M	Mach number
m	Coefficients used in spline function
N	Number of strips; also number of points
P	Static pressure normalized by its free-stream value
R	Local radius of curvature normalized by the chord length
S	Specific entropy
s,n	Orthogonal curvilinear coordinates measured along and normal to the airfoil surface normalized by the chord length
u,v	Velocity components in cartesian coordinates, normalized by the free-stream velocity
V_s,V_n	Velocity components along and normal to the airfoil surface, normalized by the free-stream velocity
V_ξ,V_η	Velocity components in (ξ,η) coordinates, normalized by the free-stream velocity
x,y	Cartesian coordinates normalized by the chord length
$\bar{x},\bar{y}$	Rotated cartesian coordinates normalized by the chord length
α	Angle of attack
β	Oblique shock angle

γ	Specific heat ratio
δ	Normal distance between the airfoil surface and system boundary normalized by the chord length
θ	Surface inclination angle with respect to the direction of free-stream velocity
ξ, η	Orthogonal curvilinear coordinates measured along and normal to the stagnation streamline normalized by the chord length
ρ	Static density normalized by its free-stream value
σ	Exponent used in Equation (22)
ϕ	Angle between x- and $\bar{x}$-axis
χ	Angle between streamline tangent and n-axis
ψ	Angle between stagnation streamline and x-axis

Subscripts

b	Conditions at airfoil surface
s	Slip streamline
stag	Stagnation
t	Trailing edge
δ	Conditions at system boundary
$1,2$	Conditions before and after shock wave
∞	Free-stream conditions

ABSTRACT

Numerical procedures developed in Part I of the present report for applying the method of integral relations to transonic airfoil problems are extended here to lifting cases. A modification of the strip arrangement described in Part I now enables any desired number of strips and size of integration domain to be used. The full inviscid flow equations (may be rotational) are employed and approximated by second-order polynomials in transverse direction in a physical plane. Numerical procedures including iterative processes for solving subject two-point boundary value problems are formulated for the case of high subsonic free-stream Mach numbers. Cartesian coordinates are employed except near the leading edge region where the use of a body coordinate system is convenient to account properly for large slope variation there. The geometry of the airfoil is represented by cubic spline functions when a closed airfoil relation is not available. The effect of change of entropy across the embedded shock wave is examined by allowing a decrease in total pressure after the shock wave along the surface streamline. With the shock angle as a free parameter, oblique shock relations as well as normal shock relations can be incorporated in the solution.

Results are presented for supercritical flows past various airfoils, including two conventional, one advanced, and two shockless airfoils. Comparisons of the results with existing theoretical and/or experimental data indicate reasonably good agreements. It is found that the shock location moves forward in the case of a finite increase in entropy across the shock wave; the change of entropy has, therefore, a cumulative effect on the flow.

ADMINISTRATIVE INFORMATION

The work presented in this report was supported by the Naval Air Systems Command (AIR-320) under NAVAIR TASK R230.201.

INTRODUCTION

The problem of inviscid transonic flow past a prescribed airfoil has been studied by using numerical procedures based on the method of integral relations. The results of the investigation are reported at different stages of completion. Part I of this report presented the numerical procedures and exploratory results for flows over symmetric airfoils at zero angle of attack.[1] Since then, the method has been extended to lifting airfoils. The flows are also inviscid supercritical, with embedded shock waves. The work of this stage is now described as Part II.

Since Part I was published in September 1970, research effort on transonic flows has been phenomenal as reflected by the number of survey and/or review papers that have appeared during this interim period. A survey paper by Newman and Allison[2] lists a large number of theoretical papers relating to steady inviscid external transonic flows and provides up-to-date information for assessing the state of the art. Three review papers on theoretical methods in transonic flows have recently been published; sequentially these are by Murman,[3] Norstrud,[4] and Yoshihara.[5] The Norstrud paper summarizes available analytical and numerical methods for the solution of an appropriate transonic flow problem and covers a broad range of transonic flows. The papers by Murman and Yoshihara, on the other hand, are more or

---

1. Tai, T.C., "Application of the Method of Integral Relations to Transonic Airfoil Problems: Part I - Inviscid Supercritical Flow over Symmetric Airfoil at Zero Angle of Attack," NSRDC Report 3424 (Sep 1970); also presented as Paper 71-98, AIAA 9th Aerospace Sciences Meeting, New York, N.Y. (Jan 1971).

2. Newman, P.A. and D.O. Allison, "An Annotated Bibliography on Transonic Flow Theory," NASA TM X-2363 (Sep 1971).

3. Murman, E.M., "Computational Methods for Inviscid Transonic Flows with Imbedded Shock Waves," Boeing Scientific Research Laboratories Document D1-82-1053 (1971); also presented in AGARD-VKI Lecture Series on Numerical Methods in Fluid Dynamics, Rhode-Saint-Genese, Belgium (Mar 1971).

4. Norstrud, H., "A Review of Transonic Flow Theory," Lockheed-Georgia Company, Report ER-11138(L) (Aug 1971); also presented as Paper at University of Illinois Seminar (Mar 1971).

5. Yoshihara, H., "Some Recent Developments in Planar Inviscid Transonic Airfoil Theory," AGARDograph 156, North Atlantic Treaty Organization (Feb 1972).

less confined to the area of computational methods. The former treats existing methods for flows with embedded shock waves. The latter is concerned with the hodograph method for shockless flows and finite difference schemes for more general flows. Both papers emphasize methods based on the use of finite difference procedures.

The method of finite differences is a highly developed numerical procedure. It is generally not difficult to select a difference scheme to approximate the differential equations in a stable manner, and the method is well suited for application to transonic flow problems. An example is the time-dependent approach of Magnus and Yoshihara.[6] The computations are lengthy, however. It is more economical to use small disturbance equations with relaxation procedures, as employed by Murman and Cole.[7] The disadvantage of using these equations, however, is that they preclude the important class of airfoils with blunt noses and these are currently of interest.* Steger and Lomax[8] employed a more realistic system consisting of inviscid, fully nonlinear, potential flow equations. Their approach proved to be fruitful; its only drawback was that the system of equations used does not allow an entropy (or total pressure) change across the shock wave. Although the change of entropy is normally small in transonic flows, it may influence the location of the shock wave (because of the change of the downstream conditions), and thus alter a considerable portion of the entire flow. This point is sometimes overlooked.

Because of the various difficulties involved in using finite difference

---

*In a private communication, however, Dr. Murman indicated that although the small disturbance equations were not valid for blunt-nosed airfoils, his overall result was surprisingly not greatly affected by nose bluntness.

6. Magnus, R. and H. Yoshihara, "Inviscid Transonic Flow over Airfoils," General Dynamics/Convair Division Report (1969); also presented as Paper 70-47, AIAA 8th Aerospace Sciences Meeting, New York, N.Y. (1970).

7. Murman, E.M. and J.D. Cole, "Calculation of Plane Steady Transonic Flows," AIAA J., Vol. 9, No. 1, (Jan 1971), pp. 121-141 (AIAA Paper No. 70-188, 1970).

8. Steger, J.L. and H. Lomax, "Numerical Calculation of Transonic Flow About Two-Dimensional Airfoils by Relaxation Procedures," presented as AIAA Paper 71-569 at AIAA 4th Fluid and Plasma Dynamics Conference, Palo Alto, California (Jun 1971).

schemes, it is natural to take an alternative approach, such as the method of integral relations (MIR) employed in the present report. Other recent applications of the method to transonic flows past airfoils include those by Holt and Masson,[9] Melnik and Ives,[10] and Sato.[11] However, these studies are confined to subcritical flows or supercritical flows over symmetric shapes using only two strips.

In the present report, the basic numerical procedures described in Part I are extended to lifting arbitrary shapes and subsequently refined. The enforcement of the Kutta condition is accomplished by adding one more iteration to the previous procedures. The use of full inviscid non-isentropic equations allows an entropy change across the shock wave. The airfoils considered include two conventional airfoils, two shockless airfoils, and one advanced (supercritical) airfoil, all at supercritical flow conditions corresponding to $M_\infty < 1$ transonic regime.

BASIC FLOW EQUATIONS

The basic flow equations for the lifting cases are the same as those used in Part I except that nonisentropic jump is introduced across the shock wave. For the sake of convenience, they are repeated here

Continuity:

$$\frac{\partial(\rho u)}{\partial x} + \frac{\partial(\rho v)}{\partial y} = 0 \qquad (1)$$

---

9. Holt, M. and B.S. Masson, "The Calculation of High Subsonic Flow Past Bodies by the Method of Integral Relations," Second International Conference on Numerical Methods in Fluid Dynamics, University of California, Berkeley (Sep 1970).

10. Melnik, R.E. and D.C. Ives, "Subcritical Flows of Two-Dimensional Airfoils by a Multistrip Method of Integral Relations," Second International Conference on Numerical Methods in Fluid Dynamics, University of California, Berkeley (Sep 1970).

11. Sato, J., "Application of Dorodnitsyn's Technique to Compressible Two-Dimensional Airfoil Theories at Transonic Speeds," National Aerospace Laboratory Technical Report TR-220T (Tokyo, Japan) (Oct 1970).

x-Momentum:

$$\frac{\partial}{\partial x}(KP + \rho u^2) + \frac{\partial}{\partial y}(\rho uv) = 0 \tag{2}$$

y-Momentum:

$$\frac{\partial}{\partial x}(\rho uv) + \frac{\partial}{\partial y}(KP + \rho v^2) = 0 \tag{3}$$

These equations are written in a Cartesian coordinate system, governing a steady, adiabatic inviscid fluid flow. The lengths are normalized with respect to the chord length, and pressure, density, and velocity components are normalized with respect to their free-stream values. The symbol K represents

$$K = \frac{1}{\gamma M_\infty^2}$$

where for air, $\gamma = \gamma_\infty = 7/5$.

The boundary conditions are as follows:

At the airfoil surface, the normal velocity component is equal to zero, i.e.,

$$V_n = u \sin\theta + v \cos\theta = 0 \tag{4a}$$

where θ is the surface inclination angle with respect to the direction of free-stream velocity.

At infinity, the flow is undisturbed, i.e.,

$$P = \rho = u = 1$$
$$v = 0 \tag{4b}$$

One more equation is needed in order to determine four dependent variables u, v, ρ, and P. It is the isentropic relation between the density and static pressure

$$P = \rho^\gamma \tag{5a}$$

This is good for regions before the shock wave and the far field. For regions after the shock wave, where the fluid has a finite increase in entropy (or a decrease in the total pressure), it becomes

$$P = \mathrm{EXP}\left(\frac{S_2 - S_1}{c_v}\right) \rho^{\gamma} \tag{5b}$$

The change of entropy (S_2-S_1) is normally small for transonic flows. However, as will be discussed later because of the corresponding change of the downstream conditions, it may influence the location of the shock wave and thus alter considerable portions of the entire flow. Nonetheless, the flow behind the shock wave is still isentropic along a streamline (which serves as strip boundary). The new isentropic relation, however, is based on a new entropy level which is slightly higher than its free-stream value. The new entropy level differs from one streamline to the other because the shock strength encountered on each streamline differs.

The value of new entropy level is obtained through the following relation

$$\mathrm{EXP}\left(\frac{S_2 - S_1}{c_v}\right) = \frac{P_2}{\rho_2^{\gamma}} \tag{6}$$

where P_2 and ρ_2 are the static pressure and density immediately after the shock. For an inviscid flow, the shock is normal at the surface in order to keep the flow attached. The Rankine-Hugoniot relations for normal shock waves are appropriate here for determining P_2 and ρ_2. They are:

$$\rho_2 = \rho_1 \frac{(\gamma+1)\, M_1^2}{(\gamma-1)\, M_1^2 + 2} \tag{7a}$$

$$P_2 = P_1 \left[1 + \frac{2\gamma}{\gamma+1} (M_1^2 - 1)\right] \tag{7b}$$

Subscripts $_1$ and $_2$ respectively denote values in front of and behind the shock wave.

It is well known that the shock is curved away from the surface. Therefore oblique shock relations must be used for the intermediate strip boundary.

$$\rho_2 = \rho_1 \frac{(\gamma+1)(M_1 \sin \beta)^2}{(\gamma-1)(M_1 \sin \beta)^2 + 2} \tag{8a}$$

$$P_2 = P_1 \left[1 + \frac{2\gamma}{\gamma+1} (M_1^2 \sin^2 \beta - 1)\right] \quad (8b)$$

where β is the shock angle with respect to the local streamline direction. When β = 90 degrees, Equations (8) become the normal shock relations.

In fact, the Rankine-Hugoniot relations are contained in the system of Equations (1) - (3) if the latter are applied along a streamline. Use of the normal shock relations at the foot of the shock wave is known to be questionable. Emmons[12] found that the Rankine-Hugoniot relations lead to infinite curvature where the shock touches the curved wall of the airfoil. Sichel[13] proposed a model which accounts for the non-Rankine-Hugoniot nature of weak shocks near the wall. The Sichel model includes a viscosity term to give a system of viscous transonic equations for the non-Rankine-Hugoniot region. It is difficult to solve these equations mathematically, but it has been demonstrated that an oblique shock wave represents an exact similarity solution.

On the basis of the above arguments, therefore, the normal shock value for the shock jump condition at the foot of the shock could be in great error for certain cases. In such cases, an oblique shock jump should correlate the flow better than the normal shock jump.[14] The angle of the oblique shock, of course, cannot be resolved without considering the viscous-inviscid interaction. An empirical curve of the pressure ratio before and after the shock foot was determined by Sinnot.[15]

There are limiting cases in which the strength of the shock is so weak that it can be considered as a series of compression waves. The flow

---

12. Emmons, H.W., "Flow of a Compressible Fluid past a Symmetrical Airfoil in a Wind Tunnel and Free Air," NACA TN 1746 (Nov 1948).

13. Sichel, M., "Structure of Weak Non-Hugoniot Shocks," Physics of Fluids, Vol. 6, No. 5, pp. 653-662 (May 1963).

14. Ferrari, C. and F.G. Tricomi, "Transonic Aerodynamics," Translated by R.H. Cramer, Academic Press (1968).

15. Sinnot, C.S., "On the Prediction of Mixed Subsonic/Supersonic Pressure Distributions," J. Aerospace Sciences, Vol. 27, pp. 767-778 (1960).

is then the so-called "shockless" solutions[16-18] or the "weak solution" to the subject boundary-value problem.[19]

In order to be consistent with the inviscid model, the normal shock relations are applied in the present study at the foot of the shock wave. In some cases, options of oblique shock values are also provided with the shock angle as a free parameter. Furthermore, it is assumed that the embedded shock wave is steady under the imposed boundary conditions.

NUMERICAL ALGORITHM

METHOD OF INTEGRAL RELATIONS (MIR)

The feasibility of applying the method of integral relations to supercritical flows over symmetric airfoils at zero angle of attack has been studied and demonstrated in Part I of the present report. Necessary numerical procedures were described and a new strip arrangement was introduced which allows the free-stream condition to be set at "infinity." The approach is now extended to lifting cases.

Briefly, in applying the method of integral relations, the system of flow equations must be written in divergence form:

$$\frac{\partial}{\partial x} A(x,y,u,\ldots) + \frac{\partial}{\partial y} B(x,y,u,\ldots) = Q(x,y,u,\ldots) \qquad (9)$$

The divergence form of Equations (1) - (3) may then be integrated outward from the airfoil surface (but not necessarily normal to the surface) to each strip boundary successively at some constant value of x. This

---

16. Nieuwland, G.Y., "Transonic Potential Flow around a Family of Quasi-Elliptical Aerofoil Sections," National Aerospace Laboratory (Amsterdam) Technical Report T-172 (Jul 1967).

17. Korn, D.G., "Computation of Shock-Free Transonic Flows for Airfoil Design," New York University Courant Institute of Mathematical Sciences, Report NYO-1480-125 (Oct 1969).

18. Boerstoel, J.W. and R. Uijlenhoet, "Lifting Airfoils with Supercritical Shockless Flow," ICAS Paper 70-15, 7th Congress of the International Council of the Aeronautical Sciences, Rome, Italy (Sep 1970).

19. Morawetz, C.S., "The Dirichlet Problem for the Tricomi Equation," Convn. Pure Appl. Math, Vol. 23, pp. 587-601 (Jul 1970).

procedure reduces the partial differential equations (with independent variables of x and y) to ordinary ones (with independent variable x) In order to perform the integration, the variation of integrand along y must be known. A general approach is to approximate the integrands by interpolation polynomials, for example, A by

$$A = \sum_{k=0}^{N} a_k(x)(y - y_o)^k \tag{10}$$

where N is the number of strips and a_k are constants evaluated at strip boundaries. In principle, the actual flow variation may be represented more closely by an increasing number of strips.

Ordinary differential equations derived by using a second-order polynomial were presented in Part I. These equations are also used to calculate lifting cases in the present report. In the lifting case, however, they are applied separately for both upper and lower flow fields. The division of the flow fields will be discussed later.

In order to examine higher order effect in the MIR, a set of ordinary differential equations is derived by using a regular third-order polynomial. The system was coded first for the computation of upstream flow. The use of third-order equations was found to be less stable than second-order equations. This instability is attributed to a negative value of dv/dx generated in the first few steps of integration in the upstream region. This negative dv/dx is contradictory to physical phenomenon and entirely caused by the mathematical inflection point of the third-order polynomial. Not every third-order polynomial has an inflection point. However, it easily becomes inflected if the (third-order) polynomial is representing a transverse flow variation from the undisturbed free stream (straight line) to a disturbed state. Possibly it would have worked better than the second-order equations in other flow regions, but in any event, the computation has to start from the upstream region. Complexity is another unpleasant feature of third-order equations. For these reasons, they are no longer employed.

COORDINATE SYSTEMS

Similar to the nonlifting case, Cartesian coordinates are employed as the basic coordinates. In the leading edge region where drastic changes of body slopes are involved, a body-oriented orthogonal curvilinear coordinate system is incorporated. The latter is embedded in the former (Figure 1). The solution of the outer region interacts with that for the inner region. Since the width of the inner region is normally fairly thin, one-strip approximation is used in this region. Part I of this report presented ordinary differential equations reduced by using one-strip approximation in the orthogonal curvilinear coordinates. The system is revised in Part II by the addition of a momentum equation to account for the effect of body properties on the outer flow. The present forms are given in Appendix A.

There are two reasons for using the above coordinate systems in the physical plane. First, the method of integral relations is a universal numerical method. If no particular advantage can be secured by using any sophisticated transformation, convenience surely should prevail. This is particularly so when modern high-speed computers are available. Second, in calculations of supercritical flows where there are mixed (elliptic-hyperbolic) flow characters, it is difficult to select a function as a basis of transformation to a computational plane. For example, functions based on incompressible solution (such as used by Chushkin[20-22]) become highly inadequate in the present case.

STRIP BOUNDARIES AND DIVISION OF FLOW FIELD

Even though no transformation of coordinates is involved, the free-stream boundary can still be set at "infinity" in the present study. This is implemented by a new arrangement of strip boundaries. As described in

---

20. Belotserkovskii, O.M. and P.I. Chushkin, "The Numerical Solution of Problems in Gas Dynamics," "Basic Developments in Fluid Dynamics," Vol. 1, edited by M. Holt, Academic Press (1965).

21. Chushkin, P.I., "Subsonic Flow of a Gas past Ellipses and Ellipsoids," Translation of Vychislitel'naya Maternatika (USSR), No. 2, pp. 20-44 (1957).

22. Chushkin, P.I., "Computation of Supersonic Flow of Gas past Arbitrary Profiles and Bodies of Revolution (The Symmetric Case)," Translation of Vychislitel'naya Maternatika (USSR), No. 3, pp. 99-110 (1958).

Part I, the idea is to treat the whole integration domain as a series of different effective regions; a small number of strips may be used within each region. The whole integration domain with free-stream as its outer boundaries can be set as large as desired. It then corresponds to an application of the free-stream boundary at "infinity." A significant advantage of this new arrangement, however, is that it allows the use of a large number of strips without the need for higher order polynomials which usually cause numerical difficulties in actual computation.

Similar to nonlifting cases, some typical streamlines are used as strip boundaries in the present approach. In the lifting case, however, the upper and lower flow fields are divided by the streamline passing along the airfoil surface. In the upstream region, this streamline is called the stagnation streamline. It splits into the upper and lower surfaces of the airfoil on striking at the stagnation point and meets again at the trailing edge (for the present inviscid flow). After leaving the trailing edge, it flattens out and asymptotically approaches an undisturbed state far downstream.

The equations for determining the stagnation streamline geometry are derived by using a procedure similar to that presented earlier.[23] They are given below.

$$\frac{Dx}{D\xi} = \cos\ \psi \tag{11a}$$

$$\frac{Dy}{D\xi} = \sin\ \psi \tag{11b}$$

$$\frac{D\psi}{D\xi} = \frac{1}{\gamma M^2 P}\left(\sin\ \psi\ \frac{\partial P}{\partial x} - \cos\ \psi\ \frac{\partial P}{\partial y}\right) \tag{11c}$$

The geometry of a typical stagnation streamline is shown in Figure 2.

Five strips are used in the far field of the upstream region and eight in the near field of this region for both upper and lower sides. Six strips are employed for the leading edge region including the strip associated with the orthogonal curvilinear coordinates. The number may

---

23. Tai, T.C., "Streamline Geometry and Equivalent Radius over a Flat Delta Wing with Cylindrical Leading Edge at an Angle of Attack," NSRDC Report 3675 (Oct 1971).

be reduced to five in case the sonic line might touch the nearest strip boundary. Four or five strips are mostly used for the airfoil region depending on the flow condition or the local airfoil curvature. In the downstream region, the number of strips can even be decreased to three. The outermost strip boundary (free-stream) is set about seven chord lengths away from the airfoil. The above strip arrangement is based somewhat on a compromise between accuracy and numerical instability. An important factor for the setup of course is that it allows the recovery of the free-stream values in the far downstream for the sake of existence and uniqueness of the solution as discussed later. The schematic view of the strip arrangement is shown in Figure 1.

AIRFOIL REPRESENTATION BY SPLINES

In analyzing transonic lifting airfoil problems by using the method of integral relations, difficulty has been encountered in obtaining continuous first- and second-order derivatives of the airfoil surface. This is because only tabulated coordinates are available for airfoils other than the NACA four-digit family. In the process of numerical solution, those tabulated coordinates must be transformed to a curve through the curve-fitting technique. Of the various techniques available for numerical interpolation, the cubic spline function was found to be best suited for curve-fitting purposes because the function and its first- and second-order derivatives are continuous in the whole range.[24] Accordingly, the cubic spline function is employed for representing arbitrary airfoils.

Equations of the cubic spline function used for airfoil representation are presented in Appendix B.

NUMERICAL INTEGRATION

With the partial differential equations reduced to a set of ordinary differential equations by the method of integral relations, the numerical integration may be carried out along the longitudinal axis x by using a standard scheme such as the fourth-order Runge-Kutta method. The details of the integration for each region are described below.

---

24. Ahlberg, J.H. et al., "The Theory of Splines and Their Applications," Academic Press (1967).

Integration in Upstream Region

The numerical integration first starts from the upstream region sufficiently far away ahead of the airfoil, say, approximately four chord lengths. Integrations for both upper and lower flow fields are carried out simultaneously. Physically, the uniform flow here is disturbed by the presence of the airfoil. The velocity will decrease along some streamlines and increase along others. In particular, the velocity along the stagnation streamline will monotonically decrease to zero. Thus, the behavior of the stagnation streamline provides a constraint in determining the flow field in the upstream region. Once the velocity along the stagnation streamline decreases, the whole upstream flow field ought to vary accordingly. This concept is implemented in our computation in order to create the flow variation far upstream. Practically, the velocity along the stagnation streamline is forced to decrease by applying an artificial disturbance* in the beginning of the integration. After a few steps, a transverse velocity gradient along the stagnation streamline is created by the overall flow field. It causes the velocity along the stagnation streamline to decrease. As soon as the system begins to work stably, the artificial disturbance is taken away.

The integration for the upstream region ends at a station in front of the airfoil. The flow along the stagnation streamline is further extrapolated to the stagnation point with a third-order Lagrange polynomial:

$$u(x) = \sum_{i=0}^{3} L_i(x) u_i \tag{12a}$$

where $L_i(x)$ is the Lagrange multiplier function

$$L_i(x) = \frac{(x-x_0)(x-x_1)\ldots(x-x_{i-1})(x-x_{i+1})\ldots(x-x_N)}{(x_i-x_0)(x_i-x_1)\ldots(x_i-x_1)(x_i-x_{i+1})\ldots(x_i-x_N)} \tag{12b}$$

At this stage a test is made to determine whether the flow along the airfoil will become supercritical or subcritical.

---

*This artificial disturbance is not an arbitrary one, however. Its form and strength are determined by satisfying the terminal condition at the stagnation point. The procedure involves an iteration process which will be discussed later in greater detail.

Supercritical or Subcritical Test

The present study considers supercritical flows over a lifting airfoil. The flow over the upper surface of the airfoil will be supercritical while that over the lower surface usually remains subcritical. The great majority of transonic airfoil flows fall into this category. Quite often, however, flows over both sides of the airfoil can be either supercritical or subcritical, depending on the free-stream Mach number and angle of attack. Thus, we have to determine which side of the airfoil will have supercritical or subcritical flows before we proceed with the numerical integration along the airfoil surface.

The test is based on the control surface in the leading edge flow field (Figure 3). Some approximate values of V_{s_b} at several points away from the stagnation point are determined by the law of conservation of mass in the control surface. For the control surface abcd, the mass flux entering line cd should equal to the mass flux leaving line bc, i.e.,

$$\int_d^c \rho u dy = \int_b^c \rho V_s dn \tag{13}$$

The integration of the left-hand side is performed easily since the distribution of ρu along line dc is known. The integral on the right-hand side, however, has to be approximated by a linear distribution in ρV_s:

$$\int_b^c \rho V_s dn \simeq \frac{\delta}{2} (\rho_b V_{s_b} + \rho_c V_{s_c}) \tag{14}$$

where ρ_c and V_{s_c} are known quantities at point c. Upon equating Equations (13) and (14) we obtain

$$V_{s_b} \simeq \left(\frac{2}{\delta} \int_b^c \rho u dy - \rho_c V_{s_c} \right) / \rho_b \tag{15a}$$

where ρ_b is determined by the law of conservation of energy with the aid of isentropic relations:

$$\rho_b = \frac{C - V_{s_b}^2}{C - 1}^{\frac{1}{\gamma-1}} \tag{15b}$$

and

$$C = 1 + \frac{2}{(\gamma-1)M_\infty^2} \tag{15c}$$

Note that Equation (15b) is good only for the flow before the shock wave.

The procedure is repeated to determine V_s values at points b_1, b_2, and b_3 (Figure 3). The resulting values are then extrapolated with the third-order Lagrange formula to certain distances downstream to determine whether it will become supercritical or subcritical. The same procedure is employed for the lower side of the flow.

A typical example for this test is demonstrated in Figure 4 which shows the result for an NACA 0015 airfoil at $M_\infty = 0.729$ at $\alpha = 4$ degrees. Broken lines indicate extrapolated values. If the flow is supercritical, the extrapolated M_b should exceed unity. Otherwise, it remains subcritical (Figure 4).

The error of linear approximation of Equation (14) becomes greater as the distance between the two ends δ increases. As indicated in Figure 3, the lower side certainly suffers greater error than the upper side. In any case, it is just a preliminary test to choose options relative to supercritical or subcritical flow for computations along the airfoil surface. The results of the present test have no significance for the computations given below.

Integration along Airfoil Surface

The above test indicates which side of the airfoil will be supercritical or subcritical. The present study is primarily concerned with supercritical flows; subcritical flow is considered as a special case which may happen over the lower surface of the airfoil. The basic equations to be used, however, are common for both flows. For the leading edge region, both flows use a mixed system which consists of equations associated with Cartesian coordinates for the outer portion and orthogonal curvilinear

coordinates for the inner portion. The mixed system is used in order to account for large surface derivatives in the leading edge region.

Initial Values. The numerical integration along the airfoil surface starts from a constant x-axis where the upstream region integration ended. In a mixed system formulation, this constant x-axis location is connected by a straight line normal to the airfoil surface. As an illustration, it is the line bc in Figure 3. The constant x-axis is x_0-axis. The point at the foot of this normal line corresponds to the "initial point" at the airfoil surface. That is point b in Figure 3. The distance between the x_0-axis and the airfoil stagnation point δ is not known in advance. It can be roughly determined by extrapolating the stagnation streamline to the stagnation point as mentioned previously.

The precise determination of δ_0 involves another iteration process which will be discussed in detail in the next section. Once this distance is determined, it is a simple matter to find the initial values at the initial point. This is accomplished by integrating the one-strip equations in the inner stagnation region (Figures 1 and 3) to the initial point. No difficulty is encountered in performing the integration since all values are known along the system boundary (line cd in Figure 3). The effect of inaccuracies introduced by the one-strip approximation here will be absorbed in the process for determining the distance δ_0 as discussed later.

Sonic Point. The integration of the mixed system now proceeds. The velocity along the surface accelerates rapidly. In order to avoid divergence of numerical results at the singular point, the integration of the inner system is replaced by a curve fit in the neighborhood of the sonic point. This is accomplished by using a third-order Lagrange polynomial. The singular behavior near the sonic point will be discussed in the next section. The integration continues after the sonic point (at the airfoil surface). Now there is a small supersonic region near the airfoil surface. As soon as the surface slopes become moderate, the mixed system is replaced by the regular Cartesian system. As the supersonic region grows, the sonic line might touch the first-strip boundary. In this case, that strip boundary is dropped in order to avoid numerical difficulty there.

The integration is then operated at one less number of strips.

Shock Wave. The supersonic region is generally terminated by a shock wave. If the strength of the shock wave is strong enough, the flow should be back to subsonic again. If it is weak, the flow may still remain in the supersonic state or in the subsonic state but further expand to supersonic again. In this latter case, the occurrence of multiple shock waves is possible. The method of integral relations, as formulated, allows only one shock wave to appear. This is because the uniqueness condition has to be satisfied, as discussed in the next section. For a given shock wave location, the shock wave relations are applied along the surface streamline. The shock wave is not inserted on other strip boundaries since the supersonic region for (supercritical) flows of practical interest is not tall enough to reach the existing first-strip boundary; fewer strips are needed from the sonic region on, and therefore the first-strip boundary can be set as high as 0.7 chord lengths away. This height of the first-strip boundary almost covers all supercritical flows of practical interest. For instance, shockless flows generally have a larger supersonic pocket (due to the "peaky pressure distribution") than those with an embedded shock. The following is a survey on the tallest supersonic region from existing shockless solutions:

Tallest Supersonic Region (chord length, c)	Source
0.250	Nieuwland[16]
0.545	Korn[17]
0.254	Boerstoel and Uijlenhoet[18]

There is no solution that has a supersonic region even taller than 0.6c. The determination of the shock location involves another iteration which is explained in the next section.

An important advantage of the method of integral relations is its flexibility in applying the shock wave relations. Here one can use the normal shock relations, Equations (7), or the oblique shock relations, Equations (8). After the shock wave, one can use Equation (5a) for a potential flow solution or Equation (5b) for a nonisentropic solution.

The overall effects of the entropy change across the shock wave and the shock angle on the flow can therefore be easily examined, although this is difficult to do in other existing methods. The change of entropy is third-order in $(M_1^2 - 1)$, but its effect on the flow is cumulative because of its influence on the shock location.

Right after the shock wave, the numerical integration continues. There is a short expansion of the flow because of change of airfoil curvature. This is then followed by a deceleration region down to the trailing edge. If the airfoil curvature changes appreciably in this region, one more strip may be added to get the desired sensitivity.

Kutta Condition. When the numerical integrations along the upper and lower surface reach at the trailing edge, their resulting static pressure should be equal. This is the Kutta condition for a sharp trailing edge. Unlike the relaxation technique, no apparent circulation term is treated in the present formulation. Circulation exists, of course, in the sense of different velocity distributions along the upper and lower surfaces of the airfoil. The requirement of equal pressures at the trailing edge from both upper and lower surface integrations involves another iteration process which will be given in the next section.

Subcritical Flow. As mentioned above, the flow over the lower surface of the airfoil could be subcritical for a moderate supercritical flow over the upper surface. Thus, we have to provide options for subcritical flow over the lower surface of the airfoil. In this case, the problem of the singular point and the determination of the shock wave are omitted. With the exception of these simplifications, the procedure for numerical integration follows the same pattern as for the upper surface. That is, a mixed system is used for the leading edge region and a regular Cartesian system for the rest of the airfoil surface. The number of strips may also vary according to the surface curvature. The height of the outermost strip boundary is about the same as that for the upper surface. Also, the distance δ_o between the x_o-axis and the stagnation point is the same as determined for the upper surface.

The only problem with the lower surface is the inadequacy of

the one-strip approximation for the inner stagnation region. Note from Figure 3 that the distance variable δ for the lower surface is approximately 50 percent longer than that for the upper surface. The longer this distance, the less accurate the one-strip approximation. The inaccuracy is actually attributed to the fact that the ratio of this distance to the local radius of curvature is too large. In this case, a two-strip approximation should give much better results. There is no problem in deriving a set of second-order equations for this inner region, but there is difficulty in evaluating the initial conditions for the middle strip boundary. For this reason, rather than attempt to use a two-strip approximation here, a correction is made in the radius of curvature for the one-strip system, i.e., let

$$R = C_r R_b + \delta \tag{16}$$

where C_r is the correction coefficient which has values $2.0 \geq C_r \geq 1.0$. It was found that values of $C_r = 1.5$ to 2.0 were appropriate for most cases. No such correction is used for the upper surface, i.e., $C_r = 1.0$. Possibly it too needs correction for the upper surface integration. However, as mentioned before, the inaccuracies there could have been absorbed and compensated in the process of determining y_∞ or δ_0.

Integration in Downstream Region

The procedure for integration in the downstream region is somewhat the reverse of that for the upstream region. Here we expect that the integration will result in a uniform flow in the far downstream. The integration starts at the trailing edge. Although the static pressure is the same for the upper and lower surfaces at the trailing edge, the velocities are not equal because of the total pressure change at the shock wave. Therefore, a slip streamline emanates from the trailing edge. The numerical integration is carried out simultaneously for both the upper and lower flow fields with the slip streamline as the dividing boundary. In order to simplify the procedure, the shape of the slip streamline is determined in such a way that its vertical velocity component v_s vanishes asymptotically in the downstream. This kind of variation in v_s is easily represented by an exponential curve with the property of asymptotical

decay, i.e.,

$$v_s = v_t e^{-k(x-x_t)} \tag{17a}$$

and

$$\left(\frac{dy}{dx}\right)_s = \frac{v_s}{u_s} \tag{17b}$$

Therefore, the geometry of the slip streamline is:

$$y_s = \int \frac{v_t e^{-k(x-x_t)}}{u_s} dx + y_t \tag{18a}$$

where subscripts s and t denote values along the slip streamline and at the trailing edge, respectively. The constant k is determined by satisfying the gradient of v_s at the trailing edge. Therefore we find

$$k = -\left[\frac{1}{v_s}\frac{dv_s}{dx}\right]_t \tag{18b}$$

which gives positive value for k.

In principle, similar procedure as employed in the upstream region may be used. A numerical experiment shows that the above procedure ensures numerical stability in the far downstream region.

Computation Time

A typical converged run on a CDC 6700 computer takes about 45,000 storage capacity (minimum required storage for CDC 6700) and an average of 0.04 sec per step size for various strip arrangement. A total of 700-1000 steps are needed for integration from upstream to downstream. This amounts to about 30 to 40 sec for a converged run. To take account of iterations as described in the next section, the above figure has to be increased 30 to 90 times. That is, the total computation time will be somewhat between 15 min to 1 hr on the CDC 6700, including necessary iterations. The computer program was written on the basis of convenience rather than efficiency. No attempt has been made to optimize the program. It is expected that computational experience will certainly help to cut down the number of iterations.

TWO-POINT BOUNDARY VALUE PROBLEM — ITERATIONS

Mathematically, the problem of transonic flow past an airfoil is a boundary value problem. The overall solution not only has to satisfy the governing equations but is also subject to boundary conditions. When the governing partial differential equations are reduced to ordinary set by some means, such as the method of integral relations in the present study, the problem becomes a two-point boundary value problem. The general strategy for solving the subject two-point boundary value problem is the so-called initial value technique. In this technique, initial values for the integration are estimated and iterated from time to time until the imposed or terminal conditions are satisfied. The solution procedure consists of iteration processes.

Five iteration processes are involved in the present study. They are illustrated in Figure 5 and described in detail below.

ITERATION I — UPSTREAM INTEGRATION

The upstream flow is influenced by the presence of the airfoil. As mentioned in the previous section, the variation of the upstream flow initially starts through an artificial disturbance. The form of the disturbance, however, depends on the properties at the stagnation point.

With reference to the ξ, η coordinates which are conveniently employed for the orientation of the stagnation streamline (see Sketch 1),

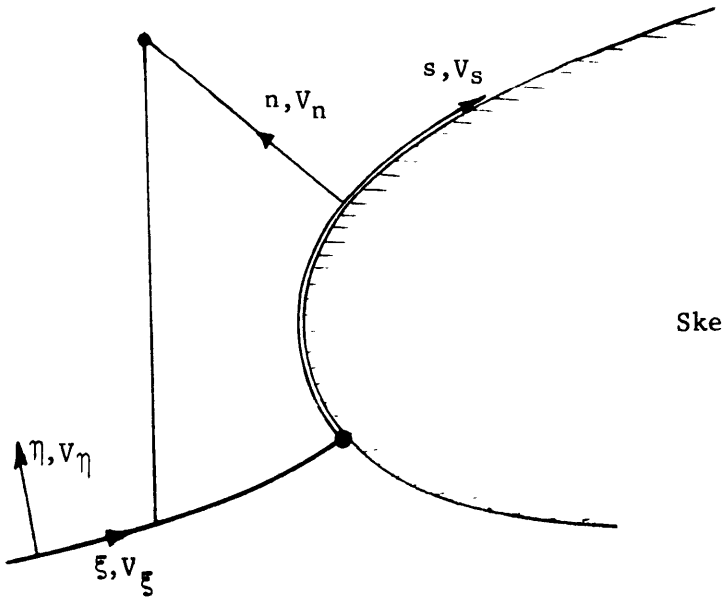

Sketch 1

the continuity and ξ-momentum equations are written as follows:

$$\frac{\partial}{\partial \xi}(\rho V_\xi) + \frac{\partial}{\partial \eta}\left[\left(1 + \frac{\eta}{R}\right)\rho V_\eta\right] = 0 \tag{19}$$

$$\frac{\partial}{\partial \xi}(\rho V_\xi^2 + KP) + \frac{\partial}{\partial \eta}\left[\left(1 + \frac{\eta}{R}\right)\rho V_\xi V_\eta\right] = -\frac{\rho V_\xi V_\eta}{R} \tag{20}$$

Note that these equations are exactly the same as Equations (A-1) and (A-2) of Appendix A if (ξ, η) coordinates are replaced by (s,n) coordinates. Along the stagnation streamline where $\eta = 0$ and $V_\eta = 0$, Equations (19) and (20) can be reduced to the following form:

$$\left(\frac{dV_\xi}{d\xi}\right)_{\eta=0} = \frac{1}{M^2-1}\left(\frac{\partial V_\eta}{\partial \eta}\right)_{\xi, \eta=0} \tag{21}$$

Equation (21) governs the velocity along the stagnation streamline. The velocity V_ξ decreases monotonically toward the stagnation point since $M < 1$ and $(\partial V_\eta/\partial \eta)_{\xi, \eta=0} > 0$. The change in V_ξ also provides a guideline for the variation of the upstream flow since the equations governing the whole upstream flow field involve V_ξ.

The disturbance is created here in terms of the transverse velocity gradient $\partial V_\eta/\partial \eta$. It then causes V_ξ to decrease. It is assumed that its magnitude in the upstream varies with its stagnation value according to a power law

$$\left(\frac{\partial V_\eta}{\partial \eta}\right)_{\xi, \eta=0} = \left(\frac{\partial V_\eta}{\partial \eta}\right)_{stag}\left(\frac{x}{x_{stag}}\right)^\sigma \tag{22}$$

For calculation purposes, a value of $\sigma = 4$ was used (a numerical experiment shows that $\sigma = 4$ is appropriate). Both $(\partial V_\eta/\partial \eta)_{stag}$ and x_{stag} are not known in advance and have to be estimated for the first time.

With the aid of Sketch 1, we find

$$\left(\frac{\partial V_\eta}{\partial \eta}\right)_{stag} \cong \left(\frac{dV_{s_b}}{ds}\right)_{stag} \tag{23a}$$

And with one-strip approximation,

$$\left(\frac{dV_{s_b}}{ds}\right)_{stag} = \frac{\rho_\delta V_{s_\delta} \frac{d\delta}{ds} - \delta_o \frac{d}{ds}(\rho_\delta V_{s_\delta}) - 2(1 + \frac{\delta_o}{R})\rho_\delta V_{n_\delta}}{\delta_o \rho_{stag}} \tag{23b}$$

Terms on the right-hand side are known after the integration reaches the x_o-axis and are extrapolated to the stagnation point. The extrapolated value for δ_o can be further improved by iteration for the singular point. The known quantities are then susbtituted into Equations (23) and the new values for both $(\partial V_\eta / \partial \eta)_{stag}$ and x_{stag} are generally different from those previously estimated. The procedure is repeated until final convergence is achieved. The significance of the iteration here is its provision of the flow feedback from the airfoil to the upstream region as characterized by elliptic equations.

As mentioned in the previous section, the disturbance is applied only for the first several steps in the upstream integration. A rapid convergence is therefore obtained for this kind of iteration. The iteration has only a slight effect on the final result. Thus it is a weak iteration.

ITERATION II – TREATMENT OF SONIC POINT

For supercritical flows, the ordinary differential equations have at least one saddle-type singularity at the sonic point(s) (or near the sonic point if the equations are written in Cartesian coordinates). This is indicated in Equations (A-4) of Appendix A (and in other du/dx equations given in Part I) where the denominator goes to zero when M = 1. Physically, however, there should be a continuous flow through the sonic point(s). A continuous solution exists only if the numerator and denominator of that equation simultaneously become zero so that the ratio 0/0 still yields a finite quantity. In order to force the numerator to zero when $M \rightarrow 1$, adjustment of certain unknown parameter(s) in the course of the solution is involved. The present iteration, therefore, adjusts certain unknown parameters (this is a common procedure for solving a two-point boundary value problem) so that a continuous solution exists at the sonic point.

It is appropriate to use the physical parameter(s) as the varying parameter(s). More than one parameter may be found to have pertinent

physical significance. At the same time, more than one strip boundary may possibly have a sonic point in the present formulation. This usually happens in the case of certain flow conditions where the sonic region crosses more than one strip boundary. In order to simplify the procedure, however, the present study considers only flows with moderate sonic region which do not cross more than one strip boundary. In fact, as discussed in the previous section, most practical flows fall into this category. As a consequence, there is only one sonic point which occurs on the surface boundary. In this case we have to choose a physical parameter as the varying parameter and fix all others, if any.

The height of the outermost strip boundary was used as the varying parameter in Part I of the present report. This outermost boundary location was introduced in Part I to modify the original infinite integration domain to a finite one.* Since the strip spacing is a function of this height, it has direct effect on the initial condition such as the velocity gradient at the initial point. Thus, it is a physical parameter. Its value will be precisely determined in the present iteration in order to obtain a continuous solution through the sonic point. The idea is analogous to the hypersonic blunt-body problem in which the adjustment of the shock standoff distance is required for a continuous solution through the sonic point (see Figure 6).

In fact, the above procedure eventually absorbs all the constituents of the inaccuracies in the initial condition for obtaining a smooth solution through the sonic point. These inaccuracies may be attributed to polynomial approximation, strip arrangement, numerical truncation, approximated values for some physical parameters, and so forth. If one of the above sources of inaccuracy is changed, the varying parameter has to be adjusted over again. Thus, determination of the unknown parameter is based on a combination of fixed values for all other extraneous and

---

*Note that the adjustment of the outermost strip boundary (free-stream boundary) does not contradict the argument for imposing the free-stream boundary as far as possible. In fact, the solution is dictated by the particular integration scheme used. For instance, the three-two-strip integration scheme allows the free-stream boundary to be imposed farther from the airfoil surface than does the two-two-strip.

physical parameters. This procedure is similar to that described by Klineberg et al.[25] in connection with the provision of unique initial conditions by requiring the correct "trajectory" to pass through the critical point. It is therefore equally valid if another physical parameter is used as the varying parameter and the others, including the outermost boundary location are fixed. The outermost boundary location is then approximately set by consideration of the accuracy of the solution.

The alternative parameter is the distance δ_o between the x_o-axis and the stagnation point. Its value has been determined by extrapolation as mentioned previously. In view of its direct effect on the velocity gradient at the stagnation point, it is a physical parameter. In this case the extrapolated value of δ_o is then adjusted such that a continuous solution exists at the sonic point.

The outermost boundary location has been used as the varying parameter in all practical computations in the present study, but it is demonstrated that the distance δ_o can be employed as the varying parameter as well. Figures 7a and 7b show the behavior of the velocity gradients near the sonic saddle point when the outermost boundary location and the distance δ_o are respectively used as the varying parameter. It is clearly seen that the end effects of both options is the same. The results indicate that it is appropriate to utilize these two parameters simultaneously as the varying parameters for handling cases where a sonic region crosses an intermediate strip boundary as well as the surface boundary. This kind of situation might happen under some extreme flow conditions.

The iteration has a marked effect on the final result. Thus, it is a strong iteration.

ITERATION III – DETERMINATION OF SHOCK LOCATION

The procedure used to determine the shock wave location in symmetric cases (as described in Part I) is extended to lifting cases. The procedure was based on a hypothesis that the shock wave location is determined by

---

25. Klineberg, J.M., et al., "Theory of Exhaust-Plume/Boundary-Layer Interactions at Supersonic Speeds," AIAA J., Vol. 10, No. 5, pp. 581-588 (May 1972).

the condition whereby the flow returns to its undisturbed state sufficiently far downstream. It is analogous to the principle of nozzle flow where the location of the shock is determined by matching the static pressure at the nozzle exit (Figure 8). In lifting cases, however, the downstream condition is checked separately for both upper and lower regions.

During the iteration process, the shock wave relations are applied at a number of assumed shock wave locations. After the shock wave, the integration resumes down to the trailing edge and finally through the downstream region. The results for each assumed shock location are then checked to determine whether the downstream boundary condition is satisfied, i.e., whether the flow based on a particular shock location approaches a uniform state in the far downstream. The shock location that meets this criterion is considered "correct" and the others "wrong."

In practical computations, however, a complete uniform flow cannot be obtained because of accumulated numerical errors. Under these circumstances, a general approach is to consider the solution satisfactory if the uniform flow value can be bracketed by two integral curves based on two shock locations. This is shown in Figure 9 where the normalized pressure distributions along strip boundaries in the upper region at $y \cong 0$, 1.75, and 3.5 are plotted for various assumed shock locations for an NACA 0015 airfoil at $M_\infty = 0.729$ and $\alpha = 4$ degrees. Attention is given to the curves based on shock locations at $x = 0.50$ and 0.51. Although the difference in the shock locations is minimal, the difference in the resulting pressures is not. It is observed that the free-stream value is bracketed in these two sets of curves. It is also interesting to note that the free-stream pressure is bracketed not only along the $y \cong 0$ boundary but also along other intermediate strip boundaries (Figures 9b and 9c). This is because the flow properties on each strip depend on each other. Any change in the $y \cong 0$ boundary causes a corresponding change on the other strip boundaries. The results imply that the downstream boundary condition is satisfied for all the strips. The actual shock location therefore lies somewhere between $x = 0.50$ and 0.51. Of course, the bracketing range can be further narrowed down to give more accurate

shock location, but there is no practical significance in doing so.

The shock location determined by the present procedure is also unique (of course, within the framework of the method). This is indicated in Figure 9 which covers pressure curves based on a wide range of shock locations. Note that there is only one pair of curves which will bracket the free-stream value, i.e., the pair based on the shock locations at $x = 0.50$ and 0.51. Again, this is true for all three strip boundaries. As a matter of fact, for all the computations in the present study, the values along intermediate strips never diverge before those along the $y = 0$ boundary. Further numerical experiments (not presented in the present report) show that the integrations along intermediate strips are always stable as the flow properties along the $y = 0$ boundary approach the free-stream value.

The above procedure is good for cases of short shock wave in which the shock wave is not tall enough to touch any intermediate strip boundary. The shock relations have been applied only along the surface boundary. For cases with extreme flow conditions in which the shock wave may cross more than one strip boundary, it is necessary to construct the shock wave so as to locate the proper place to apply the shock relations at the intermediate strip boundary. The shape of the shock wave should be determined by a trial-and-error such that the location of the shock foot will still be an effective varying parameter for bracketing the free-stream value in the downstream.

The principle behind the present iteration is that satisfaction of the downstream flow condition implies a downstream influence on the entire flow. The downstream influence propagates to the upstream throughout the whole flow field in subcritical flows (see ITERATION IV). In a supercritical flow, however, part of the influence propagates up to and stops at the shock wave because there is an embedded supersonic region in front which prevents the propagation of any influence to the upstream. In fact, since it is close to the surface, this part of the influence contributes the major portion of the downstream feedback. That is why the downstream flow is so closely affected by shock wave location. The other part of the influence propagates to the upstream through the intermediate strips where the flow is subcritical. The upstream flow is affected by this part of the influence through the adjustment of the outermost boundary location.

Therefore, the overall downstream boundary condition is satisfied by results of both the present iteration and Iteration II. The present iteration, however, makes a more direct contribution than Iteration II (which is mainly concerned with the convergence of the flow at the sonic point). If there is no embedded supersonic region, the blockage of the propagation of downstream influence along the airfoil surface is removed. The separate treatments of the sonic point (Iteration II) and the shock wave location (Iteration III) are not necessary then and the two iterations are merged to one as described in Iteration IV.

ITERATION IV — INTEGRATION FOR SUBCRITICAL FLOW

The character of the elliptic equations that describe the subcritical flow requires the downstream influence to the upstream region. In our initial value technique, this requirement is also accomplished by an iteration process.

The new iteration developed here for the integration of subcritical flow is more or less based on the ideas used in Iterations II and III. That is, if there is no embedded supersonic region, there will be no sonic critical point and no shock location problem. But the location of the outermost strip boundary still has to be determined by some means and the downstream boundary condition has to be satisfied in some way. It is quite natural then to merge Iterations II and III into a single iteration and exclude the problems associated with the supersonic region, i.e., the sonic critical point and the shock wave location. Therefore, the present iteration is concerned with the determination of an outermost boundary location that satisfies the downstream boundary condition.

During the iteration process, the outermost strip location is adjusted similarly as in Iteration II and the corresponding results downstream are checked. Similar to Iteration III, the downstream boundary condition is considered satisfied if the uniform flow value can be bracketed by two integral curves based on two outermost boundary locations. Figures 10a - 10c show an example of a case where the normalized pressure distributions in the lower region are plotted for various outermost boundary locations for an NACA 0015 airfoil at $M_\infty = 0.729$ and $\alpha = 4$ degrees. Note that the free-stream value is bracketed in curves with outermost

boundary locations at y_∞ = 7.04 and 7.06.

As mentioned previously, the integrations in the downstream region are carried out separately for both upper and lower regions. The main reason for the independent treatment of the upper and lower flow fields is that it provides a clear indication of the downstream flow trend; this is important in bracketing the free-stream values for each region. In so doing, it seems that the pressure distribution along the $y \cong 0$ strip boundary (slip streamline) is multivalued. In reality, however, those pressure distributions along the $y \cong 0$ boundary obtained from either region are for the purpose of bracketing free-stream value only; at most, they can be considered as neighboring solutions. And by the same token, the bracketed solutions from both the regions are themselves the neighboring solutions. Thus, there is no multivalued solution problem. Fortunately there is no need to find the true solution along either strip boundary in the downstream region.

ITERATION V — ENFORCEMENT OF KUTTA CONDITION

As mentioned previously, the Kutta condition is satisfied by matching the static pressures at the trailing edge from integrations along both the upper and lower surfaces. This is accomplished by changing the stagnation point at the leading edge in view of its influence on the initial conditions for both sides. During the iteration process, a stagnation point is assumed somewhere at the leading edge and, consequently, the initial conditions are calculated at respective initial points at a small distance away from the assumed stagnation point. The numerical integrations are then carried out along both upper and lower surfaces and the end result at the trailing edge is checked. If the difference in static pressures at both upper and lower sides of the trailing edge exceeds a certain specified tolerance, a new stagnation point is selected. The whole procedure is then repeated until satisfactory matching in pressure at the trailing edge is obtained. The pressure values for the above matching purpose should be those which satisfy the downstream boundary condition. That is, they should be the converged values from Iterations III and IV. Fortunately, if the specified tolerance is not too small, say somewhere between 2-3 percent, the present iteration is easily converged.

In the present procedure, therefore, the stagnation point of a lifting airfoil is determined by enforcement of the Kutta condition. The procedure differs from the usual potential flow formulation in which an explicit circulation term must be involved in lifting problems. The circulation exists in the sense that the Kutta condition is satisfied at the trailing edge. Note also that there is no vorticity at the trailing edge since the formation of vorticity is traceable to the viscosity of the fluid.

RESULTS AND DISCUSSION

Calculated results at supercritical free-stream Mach numbers are presented for two conventional, one advanced (designed for supercritical), and two shockless airfoils. Flow conditions are chosen to enable comparisons with available theoretical and/or experimental data. As a matter of fact, the typical flows used by most investigators are those that are supercritical over the upper surface and subcritical for the lower surface. Results presented in the present report, therefore, fall into this category. Of course the method is good for flow conditions with supercritical flows over both sides of the airfoil. The same is true for subcritical flows.

In all the present calculations, the outermost boundary (free-stream boundary) was set about seven chord lengths away from the airfoil. The domain of integration it covers is large enough so that the flow becomes practically undisturbed at the outermost boundary. Associated with this large integration domain, the N-2 strip integration scheme was used where N varies from 3 to 8. Since Iterations II, III, and IV are nonnegotiable, they are all carried out accordingly. Iterations I and V have been converged to within 2.5 percent.

CONVENTIONAL AIRFOILS

The two cases of conventional airfoils examined are the NACA 64A410 and the NACA 0015 airfoils. Figure 11 presents the calculated surface pressure distribution on an NACA 64A410 airfoil at $M_\infty = 0.72$ and $\alpha = 4$ degrees together with those obtained by using the unsteady finite difference scheme of Magnus and Yoshihara[6] and experimental data of

Stivers.[26] The present results compare fairly well with the experimental data except in the neighborhood of the shock wave. The disagreement there is believed to be due to a strong interaction between shock wave and boundary layer. Shock wave-boundary layer interaction is very possible since the shock wave is sufficiently strong to induce the boundary layer separation (Figure 11). The agreement between the present method and the unsteady finite difference scheme is generally good. In the unsteady finite difference scheme, however, the pressure jump across the shock wave has to be spread in several steps rather than evaluated by the Rankine-Hugoniot relations as employed in the present method.

Figure 11 also indicates that if there is an increase in entropy (or a decrease in total pressure) across the shock wave, its location moves forward. This phenomenon qualitatively agrees with nozzle flow in which the shock wave moves upstream in case of a smaller total pressure.[27] Part of the overall flow field is altered as a consequence. The problem of a cumulative nonlinear effect which grows to first order over a long distance was pointed out by Hayes.[28] Pan and Varner[29] also report in their sonic boom study that entropy has a cumulative effect which modifies the shock position. The entropy effect has been neglected in all existing theoretical methods, including Part I of the present report.

The use of mixed coordinates throughout the forward sonic region is mandatory in all the computations because the change of the first and second surface derivatives in that region becomes so drastic that the pure Cartesian system is inadequate for proper response in flow variation. As shown in Figure 11, the difference in the surface pressure obtained

---

26. Stivers, L.S., Jr., "Effects of Subsonic Mach Numbers of the Forces and Pressure Distributions on Four NACA 64A-Series Airfoil Section at Angles of Attack as High as 28°," NACA TN 3163 (Mar 1954).

27. Liepmann, H.W. and A. Roshko, "Elements of Gas Dynamics," Wiley, N.Y. (1957).

28. Hayes, W.D., "Pseudotransonic Similitude and First Order Wave Structure," J. Aero. Sci., Vol. 21, No. 11, pp. 721-730 (Nov 1954).

29. Pan, Y.S. and M.O. Varner, "Studies on Sonic Boom at High Mach Numbers," AIAA Paper No. 72-652, presented at AIAA 5th Fluid and Plasma Dynamics Conference, Boston (Jun 1972).

from these two systems is significant between x/c = 0 and 0.15.

Figure 12 compares the calculated surface pressure distribution on an NACA 0015 airfoil at M_∞ = 0.729 and α = 4 degrees with theoretical results[8] obtained by using the relaxation method and with experimental data of Graham et al.[30] In order to examine the effects of the change of entropy and the shock angle, the results are presented with options of normal shocks versus oblique shocks and zero entropy change versus finite entropy change. Although there is no rational way to determine the shock angle β without considering viscous effect at this moment, the present results are calculated with shock angle as a free parameter.

The present results show that the location of a normal shock wave moves forward in case of a finite entropy change across the shock wave. The trend agrees with that for the NACA 64A410 airfoil as previously discussed. Furthermore, by allowing an entropy change across the shock, the shock location is shifted forward for an oblique shock. The smaller the shock angle, the more forward the shock location. The same is expected to be true if there were no entropy change across the shock wave. The fact that an oblique shock wave is supposed to take place earlier than a normal shock wave has been qualitatively demonstrated by Ferrari and Tricomi.[14] See Figure 73 of their book where results of shock-foot locus were compared with the theoretical prediction of Spreiter and Alksne[31] and with the empirical correlation and experimental data of Sinnot.[15] The figure indicates that the Sinnot empirical shock locations (which correspond to oblique shocks) for various airfoils are consistently considerably more forward than the results obtained[31] by using normal shock relations. It is not surprising, of course, that experiment is in favor of the Sinnot data.

The comparisons with experimental data indicate that agreement of results for the present study is best with oblique shock β = 70 degrees

---

30. Graham, D.J., et al., "A Systematic Investigation of Pressure Distributions at High Speeds over Five Representative NACA Low-Drag and Conventional Airfoil Sections," NACA Report 832 (1945).

31. Spreiter, J.R. and A.Y. Alksne, "Thin Airfoil Theory Based on Approximate Solution of the Transonic Flow Equation," NACA Report 1359 (1958), Supersedes NACA TN 3970.

and finite entropy change. The smaller the shock angle, the better the correlation. In reality, the experimental data revealed that there is a strong viscous effect near the shock wave. The use of oblique shock options in our formulation, however, is to compensate for viscous effect. In any case, there is a lower limit of the shock angle where the flow behind the shock wave is no longer subsonic. Although subsonic flow always follows a normal shock, supersonic flow could very well follow oblique shocks and additional shock wave(s) will then be required to bring the flow to subsonic state. In this case the two or more shock waves must be treated with only one downstream condition imposed. The solution then becomes multivalued. Multishock conditions are not considered in the present work.

Compared with the theoretical predictions of the relaxation method,[8] the present method yields milder acceleration in the upper leading edge; this, in turn, avoids considerable deviation from experimental values in major portions of the flow. Moderate leading edge acceleration is a characteristic of the conventional airfoils which should be modified as suggested by Pearcey[32] to obtain peaky pressure distribution for better airfoil performance at transonic speeds. The two methods are in fair agreement for results on the lower surface of the airfoil.

ADVANCED AIRFOIL

The Pearcey experiment[32] indicates that airfoil performance at transonic speeds may be improved by exploiting favorably developed local supersonic flow through peaky pressure distribution or by using a finite thickness at the trailing edge. Airfoil designed for better performance at supercritical speeds is usually referred to as advanced airfoil. Figure 13 shows the surface pressure distribution calculated for an advanced airfoil of 17 percent thickness ratio at $M_\infty = 0.70$ and $\alpha = 1.5$ degrees.

For the upper surface, a fairly peaky pressure distribution is

---

32. Pearcey, H.H., "The Aerodynamic Design of Section Shapes for Swept Wings," in "Advances in Aeronautical Sciences," Pergamon Press, Inc., Vol. 3, pp. 277-322 (1961).

observed in the leading edge region. The trend is correct since the airfoil is designed with more bluntness than conventional airfoils. It is interesting to note that unlike conventional airfoil cases, the pressure increases all the way toward the shock wave after the peaky velocity (corresponding to pressure dip in the figure) is reached. The local supersonic flow is therefore favorably developed for reducing the shock strength that generates large drag and separation. As expected, the resulting shock wave is fairly weak. Note that the result of an oblique shock does not differ much from that of a normal shock. This is because viscous effect becomes minimal in the case of very weak shock waves. Downstream of the shock wave, the flow decelerates further toward the trailing edge.

On the lower surface, moderate acceleration of the flow takes place up to 45 percent of the chord and is then followed by a strong deceleration zone. The strong deceleration here helps generate more lift in the rear portion of the airfoil. The cusp near the trailing edge helps to bring the pressure down in order to match that of the upper surface.

SHOCKLESS AIRFOILS

The type of advanced airfoil that operates without a shock wave at supercritical speeds is referred to as a shockless airfoil. It is generated by inverse procedure (i.e., the airfoil coordinates are determined from prescribed conditions) with the aid of hodograph transformation of compressible potential flow equations. However, numerical techniques for obtaining the solution vary. For instance, Nieuwland[16] obtains numerical results for a family of quasi-elliptical airfoils through series representation of hypergeometric functions. Korn[17] and Garabedian and Korn[33] construct their solutions in terms of characteristic variables in a complex domain. The shockless arifoils studied herein use a Garabedian-Korn airfoil and a Nieuwland airfoil.

Figure 14 compares the calculated results on a Garabedian-Korn airfoil at the design condition of $M_\infty = 0.75$ with the original solution of

---

33. Garabedian, P.R. and D.G. Korn, "Numerical Design of Transonic Airfoils," in "Numerical Solution of Partial Differential Equations," Academic Press, N.Y., Vol. 2, pp. 253-271 (1971).

Garabedian and Korn,[33] the small disturbance solution of Krupp and Murman,[34] and experimental data of Kacprzynski et al.[35] In general, all three theoretical solutions agree fairly well over most portions of the airfoil surface. After the midchord, the present result starts to deviate from the original shockless solution in that here the flow starts to accelerate rather than to decelerate. The explanation for the acceleration is that the surface slopes which become negative from thereon correspond to a divergent local area for two-dimensional flow and therefore cause the local supersonic flow to expand. The negative surface slope may not generate a divergent local area only if the near-field streamlines have more negative slopes than those at the surface. This does not occur in the present case. As a consequence of this local expansion, the flow must be brought back to its subsonic state by a shock wave. Here again, both normal and oblique shock relations are applied in the computation. It is observed in the figure that the shock location moves forward as its strength decreases from a normal shock to an oblique shock. Further decrease in shock strength would have resulted in a "shockless condition" as a limit.

The experimental data were measured at slightly different free-stream Mach number and angle of attack than for the original theoretical shockless condition.[35] Nonetheless, the data exhibit considerable fluctuation near the oblique shock wave for the present calculation. These fluctuations are most likely attributable to a series of weak shocks in that region.

Finally, Figure 15 presents calculated results for a quasi-elliptical airfoil generated by the Nieuwland approach at $M_\infty = 0.7557$ and $\alpha = 1.32$ degrees. The original shockless solution tabulated by Lock[36] is also given for comparison purposes. The agreement between the two solutions

---

34. Krupp, J.A. and E.M. Murman, "The Numerical Calculation of Steady Transonic Flows Past Thin Lifting Airfoils and Slender Bodies," AIAA Paper 71-566 (1971), see also Boeing Scientific Research Laboratories Report D180-12958-1 (Jun 1971).

35. Kacprzynski, J.J. et al., "Analysis of the Flow past a Shockless Lifting Airfoil in Design and Off-Design Conditions," Nat'l. Res. Council of Canada (Ottawa) Aero Report LR-554 (Nov 1971).

36. Lock, R.C., "Test Cases for Numerical Methods in Two-Dimensional Transonic Flows," AGARD Report 575 (Nov 1970).

is good except for the occurrence of a shock wave in the present result. The explanation for this difference is very much the same as in the case of Garabedian-Korn airfoil. That is, the local supersonic flow expansion after the change of surface slope about 0.3 chord requires a shock wave in order to bring the flow back to its subsonic state. Similar to previous cases, the oblique shock wave simulates the flow better than the normal one. Further decrease in shock strength would have resulted in a shockless condition.

CONCLUSION

Application of the method of integral relations to transonic flows past lifting airfoils has been shown to be feasible through a modification of strip arrangement whereby the number of strips may be considerably higher than the order of the polynomial approximation. With the present strip arrangement, any desired number of strips and size of integration domain can be used. A second-order polynomial may be incorporated in all practical computations with reasonable accuracy by using a physical plane. The simplicity of the numerical procedure enables full inviscid rotational flow equations to be used without any difficulty.

Calculated results for supercritical flows past various airfoils, including two conventional airfoils, one advanced airfoil, and two shockless airfoils, compare fairly well with existing theoretical and/or experimental data. As expected, the present results indicate that the strength of shock wave is appreciably less for the advanced airfoil than for the conventional airfoils.

It is found that the shock location moves forward in the case of a finite increase in entropy (or a decrease in total pressure) across the shock wave. This phenomenon is in qualitative agreement with nozzle flow in which the shock wave moves upstream in case of a smaller total pressure. Since the overall flow field is altered as a result of change of shock location, the change of entropy has therefore a cumulative effect on the flow. (This has been neglected in all existing theoretical solutions, including Part I of the present report.)

Better correlation between the present theoretical results and experimental data was obtained by using oblique shock rather than normal

shock relations. The shock location is shifted forward for an oblique shock. The smaller the shock angle, the more forward the shock location.

The relatively small amount of computer running time required and the reasonably good accuracy obtainable make the present method attractive for wing design applications. Furthermore, because computer storage requirements are small, it is easy to couple the method with viscous analysis for the investigation of shock wave-boundary layer interaction problems.

ACKNOWLEDGMENT

The author wishes to thank Dr. S. de los Santos, head of the Aerodynamics Division at the Naval Ship Research and Development Center, for his suggestion of this study and his encouragement throughout all phases of the present work.

APPENDIX A

INVISCID FLOW EQUATIONS IN A BODY-ORIENTED ORTHOGONAL SYSTEM

In a body-oriented orthogonal system (s,n), the governing equations of a steady, adiabatic, inviscid flow are as follows:

Continuity:

$$\frac{\partial}{\partial s}(\rho V_s) + \frac{\partial}{\partial n}\left[\left(1 + \frac{n}{R}\right)\rho V_n\right] = 0 \tag{A-1}$$

s-Momentum:

$$\frac{\partial}{\partial s}(\rho V_s^2 + KP) + \frac{\partial}{\partial n}\left[\left(1 + \frac{n}{R}\right)\rho V_s V_n\right] = -\frac{\rho V_s V_n}{R} \tag{A-2}$$

n-Momentum:

$$\frac{\partial}{\partial s}(\rho V_s V_n) + \frac{\partial}{\partial n}\left[\left(1 + \frac{n}{R}\right)(\rho V_n^2 + KP)\right] = \frac{\rho V_s^2 + KP}{R} \tag{A-3}$$

State $$P = \rho^{\gamma} \quad \text{(before shock wave)} \tag{A-4}$$

where lengths are normalized with respect to the chord length; pressure, density, and velocity components are normalized with respect to their free-stream values; and R is the radius of curvature.

Other symbols have the same meaning as in the main text. Note that an isentropic relation has been used in place of the energy equation for flows before the shock wave.

The boundary conditions are:

At the airfoil surface, the normal velocity component is equal to zero, i.e.,

$$V_n = V_{n_b} = 0 \tag{A-5a}$$

At the system boundary,

$$\begin{aligned} V_s &= V_{s_\delta} = u_\delta \cos\theta + v_\delta \sin\theta \\ V_n &= V_{n_\delta} = v_\delta \cos\theta - u_\delta \sin\theta \end{aligned} \tag{A-5b}$$

The streamline angle, χ (see Figure 1), is geometrically related to the distance δ by the relation

$$\frac{d\delta}{ds} = \frac{1 + \frac{\delta}{R}}{\tan(\chi + \theta)} \tag{A-6}$$

The divergence form of Equations (A-1) through (A-3) may be integrated

outward from the body surface to the system boundary at some constant value of s by using the method of integral relations with one-strip approximation. This procedure reduces the partial differential equations (with independent variables s and n) to ordinary ones (with independent variable s). In performing the integration, the integrands are approximated by a linear interpolation shown below.

$$I = I_b\ (s) + \frac{n}{\delta}\left[I_\delta\ (s) - I_b\ (s)\right] \tag{A-7}$$

When Equation (A-7) is substituted in the corresponding integrands of Equations (A-1) and (A-2) and integration performed with respect to n, we obtain

$$\frac{dV_{s_b}}{ds} = \frac{(\rho_b V_{s_b} + \rho_\delta V_{s_\delta})\ \frac{1}{\delta}\ \frac{d\delta}{ds} + \frac{d(\rho_\delta V_{s_\delta})}{ds}}{\rho_b\ (M_b^2 - 1)} \tag{A-8}$$

$$\frac{dV_{n_\delta}}{ds} = \frac{V_{n_\delta}}{\delta}\ \ \frac{d\delta}{ds} - \frac{V_{n_s}}{\rho_\delta V_{s_\delta}}\ \ \frac{d(\rho_\delta V_{s_\delta})}{ds} + E \tag{A-9}$$

where

$$E = \left[\left(\frac{2}{\delta} + \frac{1}{R_b}\right)\ KP_b - \left(\frac{1}{R} + \frac{2}{\delta}\right)KP_\delta + \left(\frac{\rho_b V_{s_b}^2}{R_b} + \frac{\rho_\delta V_{s_\delta}^2}{R_\delta}\right) - 2\left(\frac{1}{\delta} + \frac{1}{R_\delta}\right)\ \rho_\delta V_{n_\delta}^2\right] /\ \rho_\delta V_{s_\delta} \tag{A-10}$$

The density at the surface ρ_b are related to V_{s_b} by Equation (15b). Basically, with known properties at the system boundary, only one equation, Equation (A-8), is needed to determine the flow along the body surface. However, Equation (A-9) is employed to account for the effect of body properties on the flow in the outer stagnation region. It relates the flows in the inner and outer stagnation regions.

APPENDIX B

AIRFOIL REPRESENTATION BY SPLINE FUNCTION

The method of splines[24] has been known as an effective method for numerical differentiation, integration, and interpolation. In view of its merit in giving continuous first- and second-order derivatives, the one-dimensional cubic spline function is employed for representing arbitrary airfoils.

To illustrate the one-dimensional cubic spline, we use the Cartesian coordinates (x;y) to represent airfoil coordinates with x as the independent variable. For the interval $0 \leq x \leq 1$, a mesh Δ of surface positions is given by (x_j, y_j) with $j = 1, 2, \ldots, N$. Then the cubic spline for this mesh yields a function $y_\Delta(x)$ which (1) is continuous with its first and second derivatives in $0 \leq x \leq 1$, (2) coincides with a cubic in each subinterval $x_{j-1} \leq x \leq x_j$, $(j = 2, 3, \ldots N)$, and (3) satisfies $y_\Delta(x_j) = y_j$, $(j = 1, 2, \ldots N)$.

Let

$$m_j = y_\Delta''(x_j) = \frac{d^2 y_\Delta(x_j)}{dx^2}$$

The cubic spline on the subinterval (x_{j-1}, x_j) is assumed to have a linear variation of the second derivative, i.e.,

$$y_\Delta''(x) = m_{j-1}\frac{(x_j - x)}{\Delta x_j} + m_j\frac{(x - x_{j-1})}{\Delta x_j} \qquad \text{(B-1)}$$

where $\Delta x_j = x_j - x_{j-1}$. By integrating the above expression and evaluating the constants of integration, the first derivative and spline function on (x_{j-1}, x_j) are

$$y_\Delta'(x) = \frac{\Delta y_j}{\Delta x_j} - m_{j-1}\left[\frac{(x_j - x)^2}{2\Delta x_j} - \frac{\Delta x_j}{6}\right] + m_j\left[\frac{(x - x_{j-1})^2}{2\Delta x_j} - \frac{\Delta x_j}{6}\right] \qquad \text{(B-2)}$$

and

$$y_\Delta(x) = y_{j-1}\frac{x_j - x}{\Delta x_j} + y_j\frac{x - x_{j-1}}{\Delta x_j} + \frac{(x_j - x)(x - x_{j-1})}{6\Delta x_j} \times$$
$$[m_{j-1}(2x_j - x - x_{j-1}) - m_j(x_j + x - 2x_{j-1})] \qquad \text{(B-3)}$$

where $\Delta y_j = y_j - y_{j-1}$. The unknowns m_j's remain to be calculated. Equating the one-sided limits of the derivatives at each interior mesh point, $y_\Delta'(x_j^-) = y_\Delta'(x_j+)$ yields

$$\frac{\Delta x_j}{6}m_{j-1} + \left(\frac{\Delta x_{j+1}}{3} + \frac{\Delta x_j}{3}m_j + \frac{\Delta x_{j+1}}{6}m_{j+1} = \frac{\Delta y_{j-1}}{\Delta x_{j+1}} - \frac{\Delta y_j}{\Delta x_j}\right.$$

$$\text{for } j = 2,3,\ldots N-1. \qquad \text{(B-4)}$$

Equation (B-4) gives (N-2) simultaneous equations in the N unknowns. Therefore, two additional conditions must be specified in order to determine all the m_j's. Additional conditions are available at both ends of the curve, i.e., the end conditions. They may be imposed in terms of slopes rather than the second derivatives themselves since the latter must be determined simultaneously to account for influence from interior meshes. The slopes at the end points can easily be found. With the end slopes on hand, the one-sided derivatives from Equation (B-2) give the relations

$$2m_1 + m_2 = \frac{6}{x_2 - x_1}\left[\frac{y_2 - y_1}{x_2 - x_1} - \left.\frac{dy}{dx}\right|_{x=x_1}\right] \qquad \text{(B-5)}$$

and

$$m_{N-1} + 2m_N = \frac{6}{x_{N-1} - x_N}\left[-\frac{y_{N-1} - y_N}{x_{N-1} - x_N} + \left(\frac{dy}{dx}\right)_{x=x_N}\right] \qquad \text{(B-6)}$$

In the case of a symmetric blunt-nosed airfoil, the term $(dy/dx)_{x=x_1}$ assumes an infinite value where x_1 corresponds to the most forward point of the airfoil. In this case, the x-y plane must be rotated to a certain angle ϕ in order to avoid the infinite derivative. The spline functions are then applied at the new plane $\bar{x}$-$\bar{y}$ according to the following relation

$$\begin{aligned} \bar{x} &= x\cos\phi + y\sin\phi \\ \bar{y} &= y\cos\phi - x\sin\phi \end{aligned} \qquad \text{(B-7)}$$

It is an easy matter to transform the coordinates back to the original x-y plane after determination of m_j's. The term $(dy/dx)_{x=x_N}$ usually has a finite value at the trailing edge. No difficulty is involved in this part.

Coupled with the end conditions, Equations (B-5) and (B-6), the system of equations for determining m_j's may then be written as

$$\left.\begin{aligned} b_1 m_1 + c_1 m_2 &= d_1 \\ a_2 m_1 + b_2 m_2 + c_2 m_3 &= d_2 \\ a_3 m_2 + b_3 m_3 + c_3 m_4 &= d_3 \\ a_{N-1} m_{N-2} + b_{N-1} m_{N-1} + c_{N-1} m_{N-1} &= d_{N-1} \\ a_N m_{N-1} + b_N m_N &= d_N \end{aligned}\right\} \qquad \text{(B-8)}$$

where a_j, b_j, c_j, and d_j are constants. This is a system of N linear equations for the m_j's, and it is of the tridiagonal matrix form. The matrix is easily solved in a digital computer. In our practical computation, the number of mesh points N up to 30 has been used. Once the m_j's are evaluated, the functions $y_\Delta(x)$, $y_\Delta'(x)$, and $y_\Delta''(x)$ can be calculated from Equations (B-1) through (B-3) for any values of x in the interval $0 \le x \le 1$.

Figure 16 shows the slopes of an NACA 64A410 airfoil at $\alpha = 4$ degrees calculated by curve-fitting techniques that used both the spline function and the piecewise least square method. Note that continuity and smoothness of the slope are insured by using the spline function. In contrast, the piecewise least square method yields discontinuous slopes. A numerical experiment reveals that two factors directly affect the result of the second derivatives in airfoil representation using splines: accuracy of the input data and the number of input data points. Airfoils generated by the inverse method, such as the hodograph method for shockless flow, do not constitute any problem with accuracy since the output coordinates can be arranged to any desired accuracy. When accurate original data points are not available, care must be exercised in selecting the number of data points.

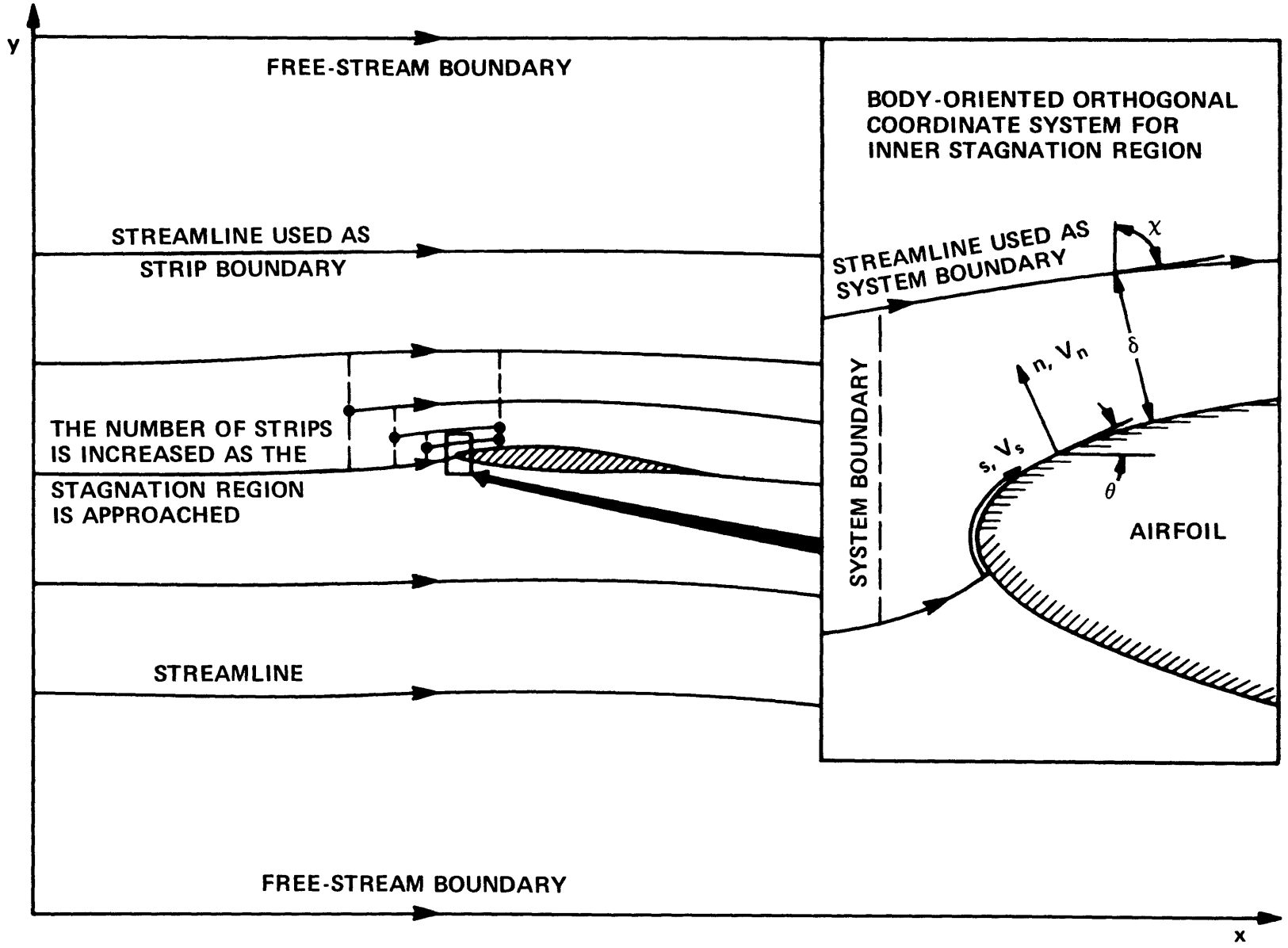

Figure 1 – Coordinate Systems and Strip Boundaries

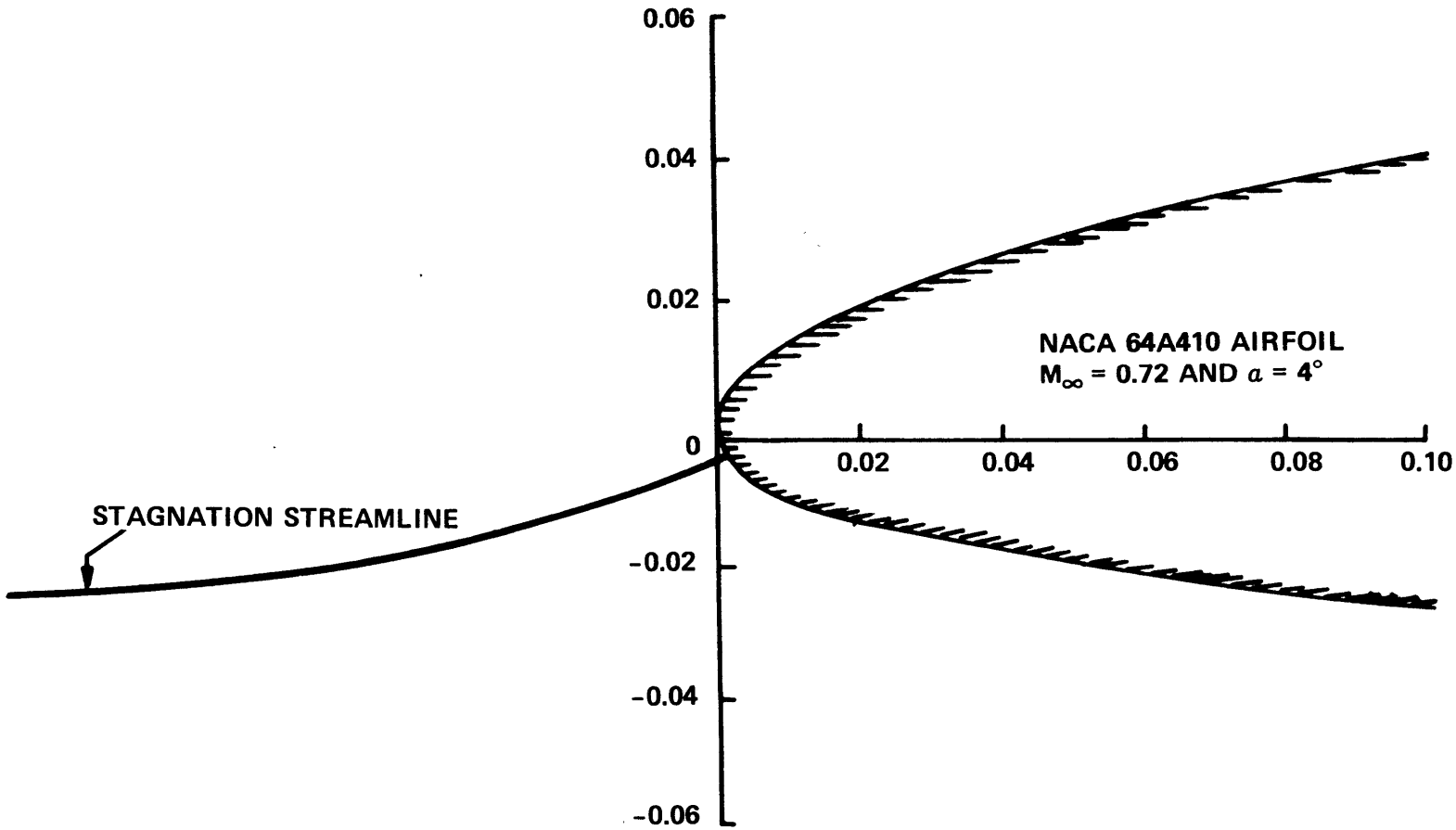

Figure 2 – Geometry of a Typical Stagnation Streamline

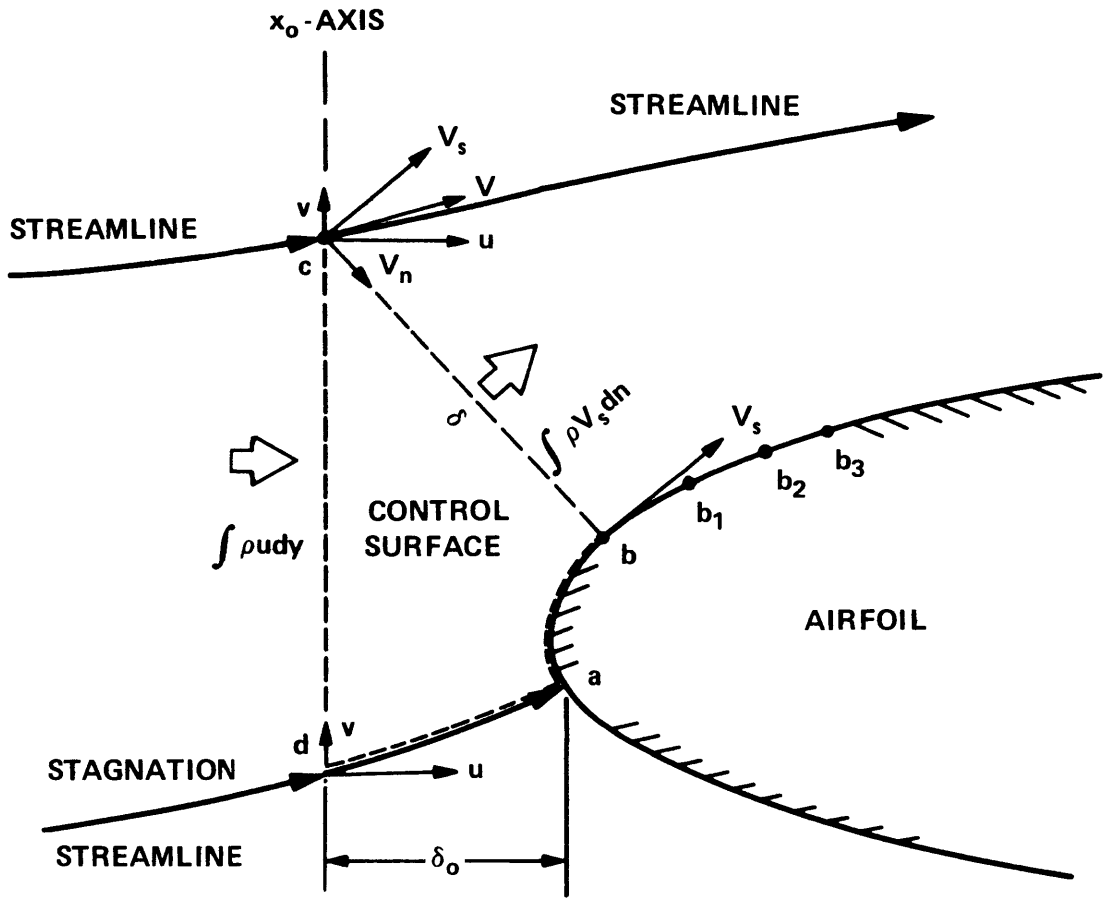

Figure 3 – A Control Surface in the Inner Stagnation Region

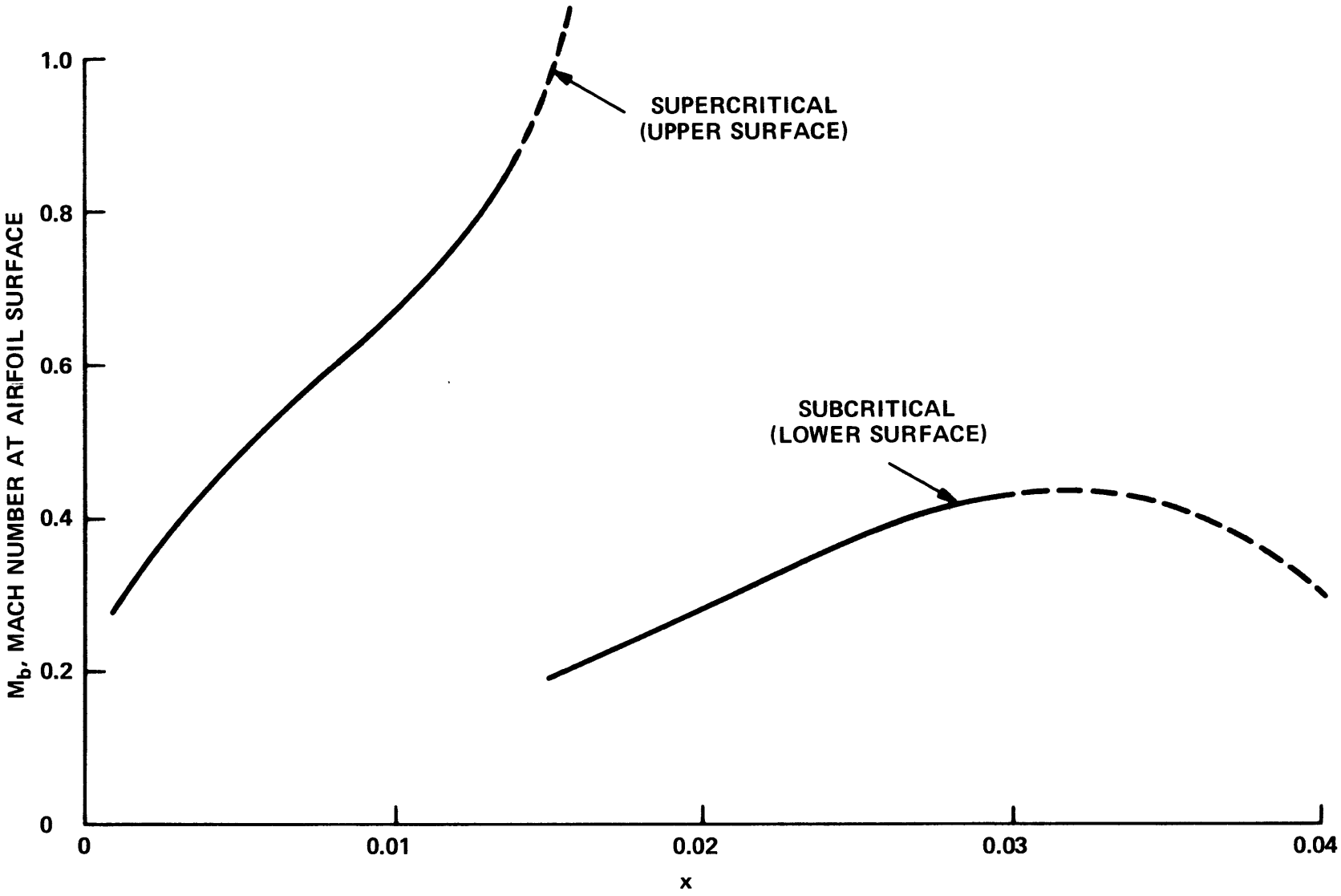

Figure 4 – Supercritical or Subcritical Test for an NACA 0015 Airfoil at $M_\infty = 0.729$ and $\alpha = 4$ Degrees

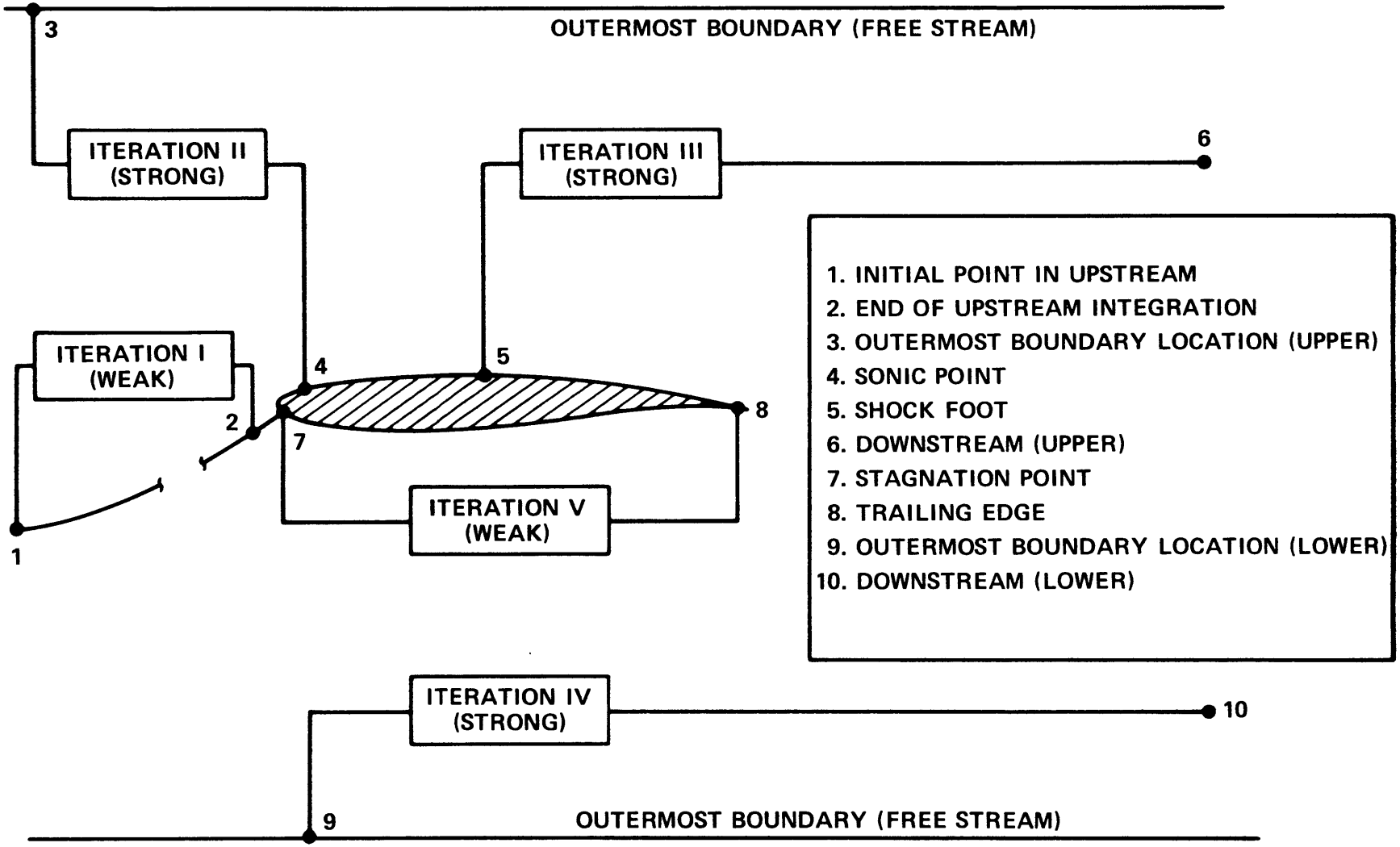

Figure 5 – Iteration Procedures for Solving Subject Two-Point Boundary Value Problems

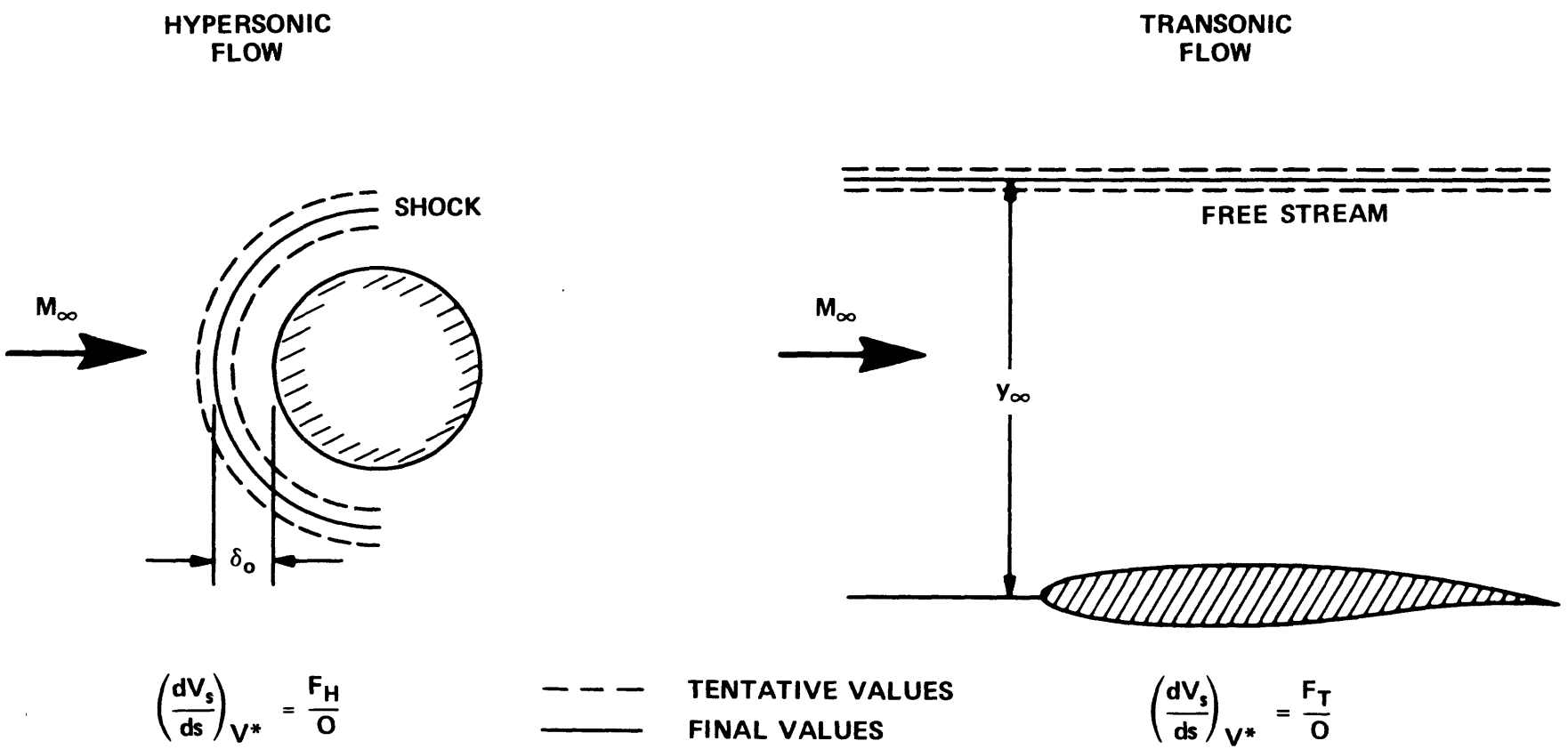

Figure 6 – Treatment of Sonic Point

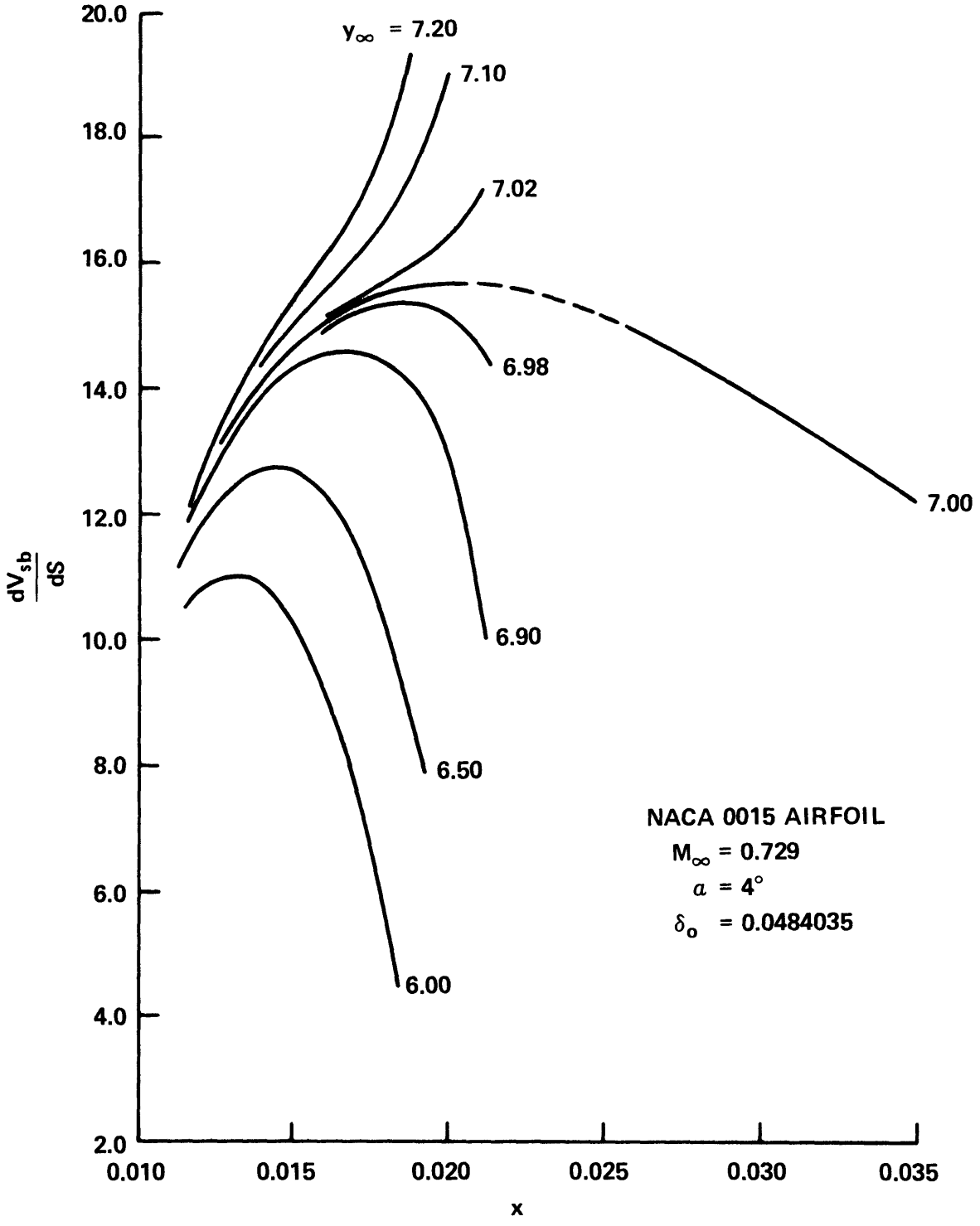

Figure 7a – Varying with Outermost Boundary Location

Figure 7 – Velocity Gradients near Sonic Point

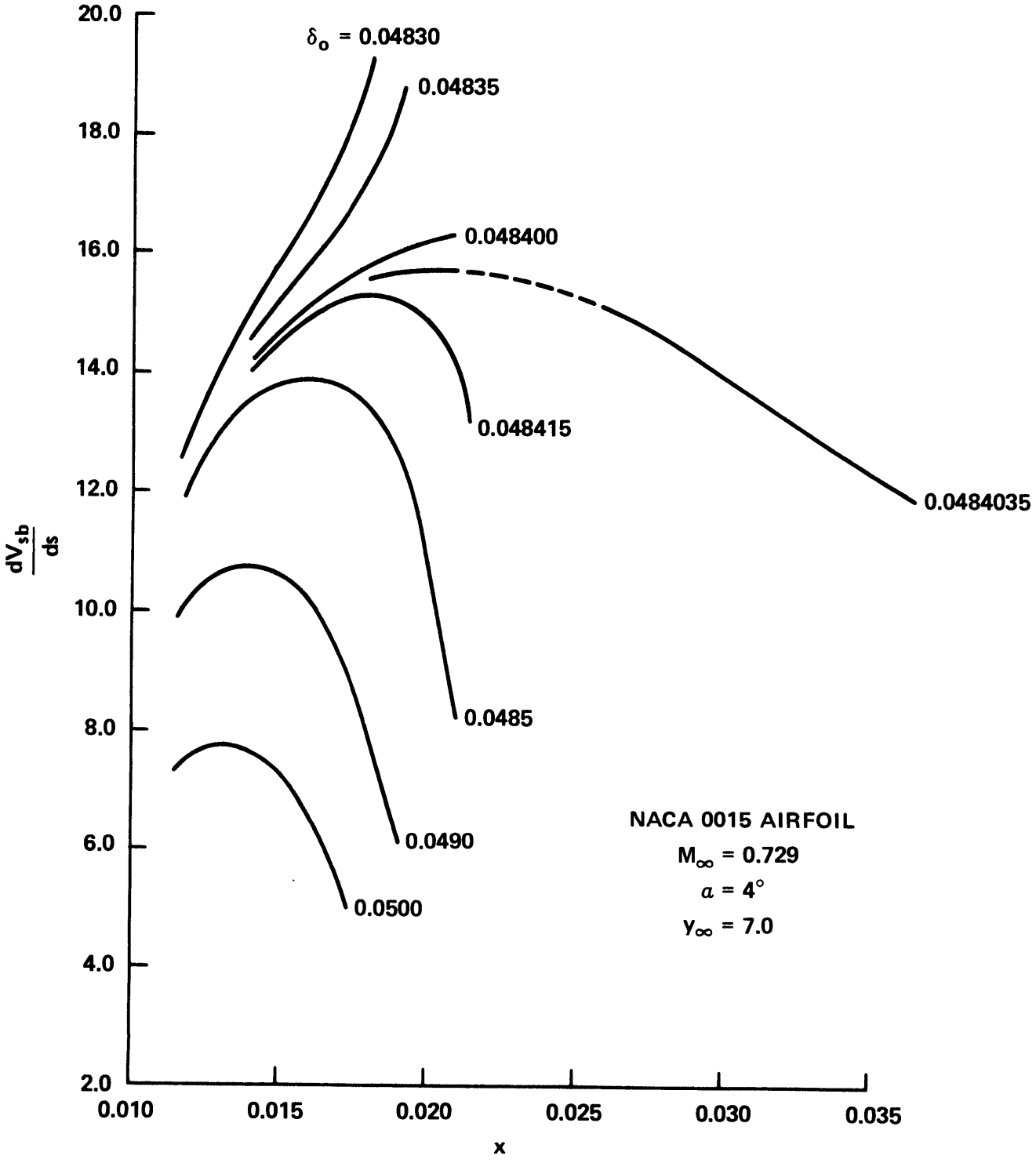

Figure 7b – Varying with Distance δ_o

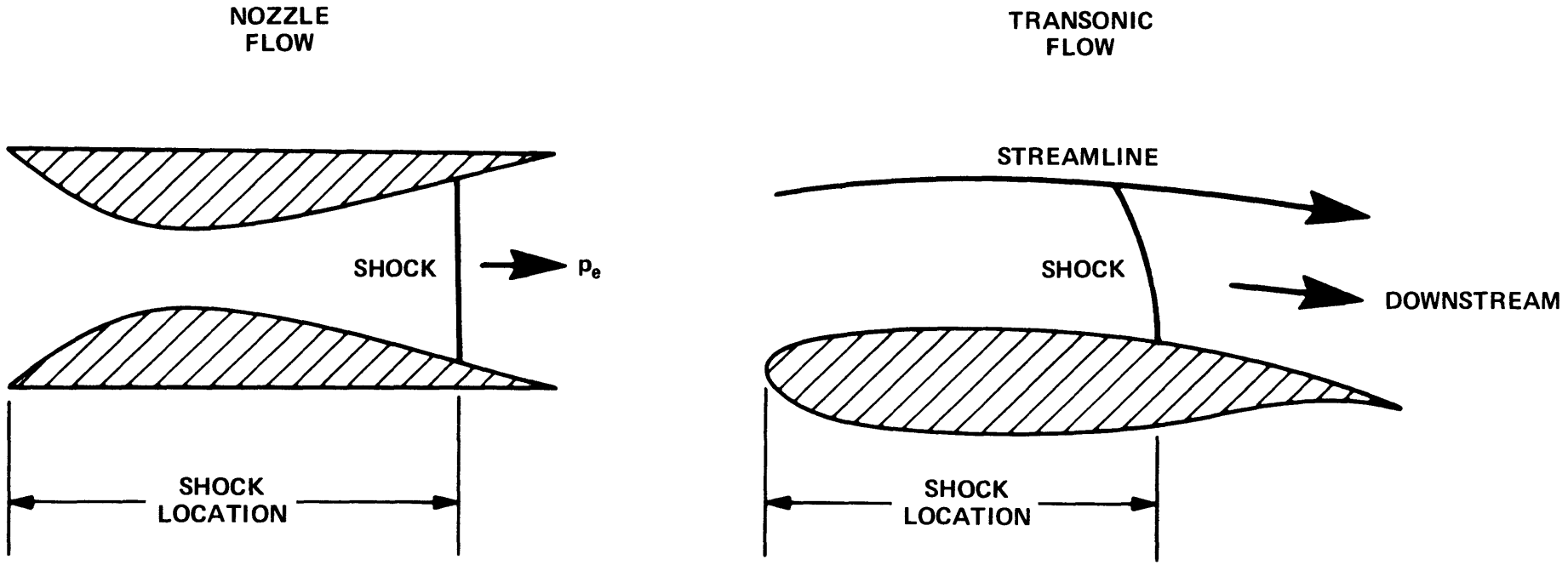

Figure 8 – Determination of Shock Location

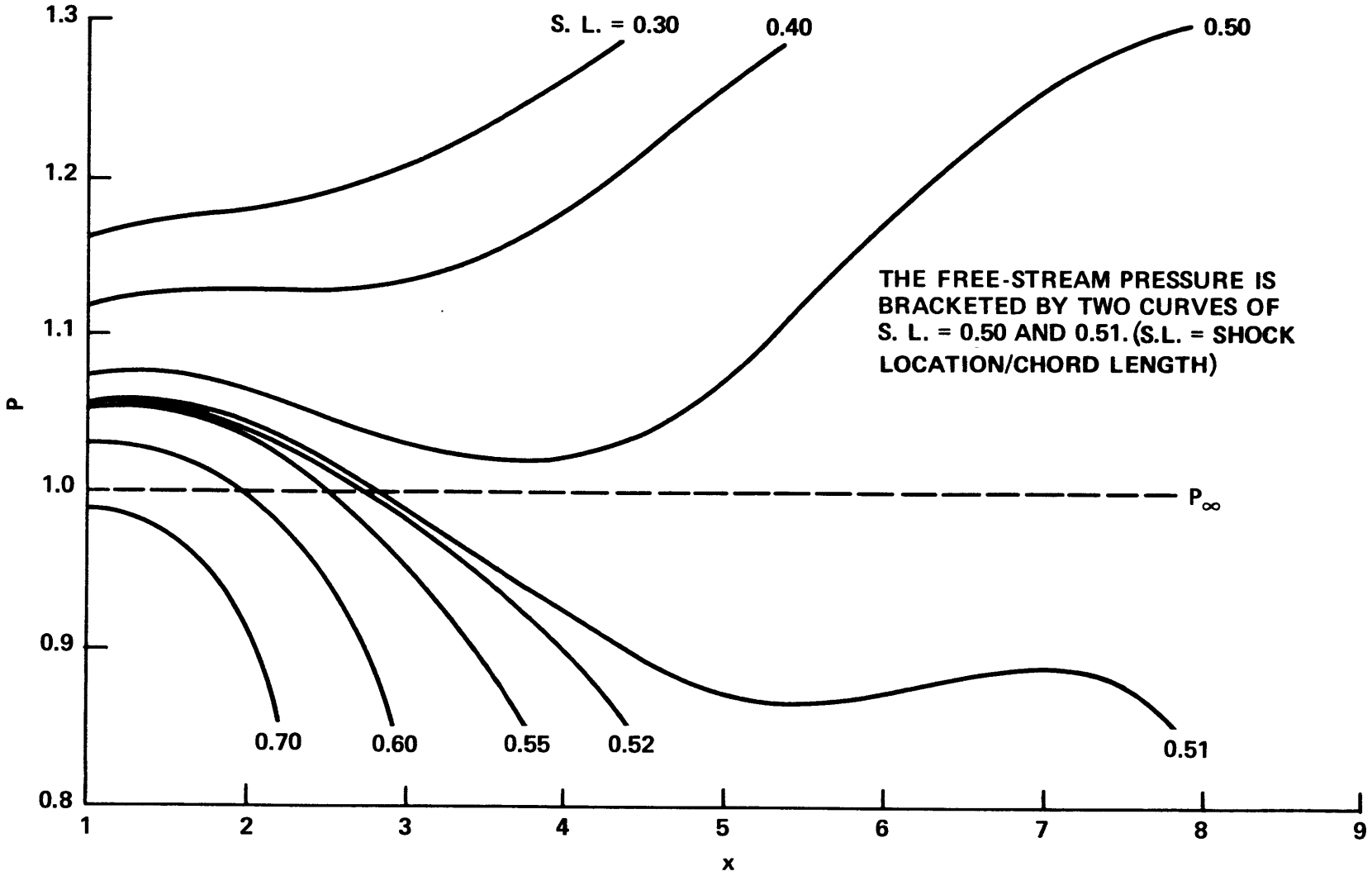

Figure 9a – $y \cong 0$

Figure 9 – Downstream Pressure Distribution in Upper Region for a NACA 0015 Airfoil at $M_\infty = 0.729$ and $\alpha = 4$ Degrees

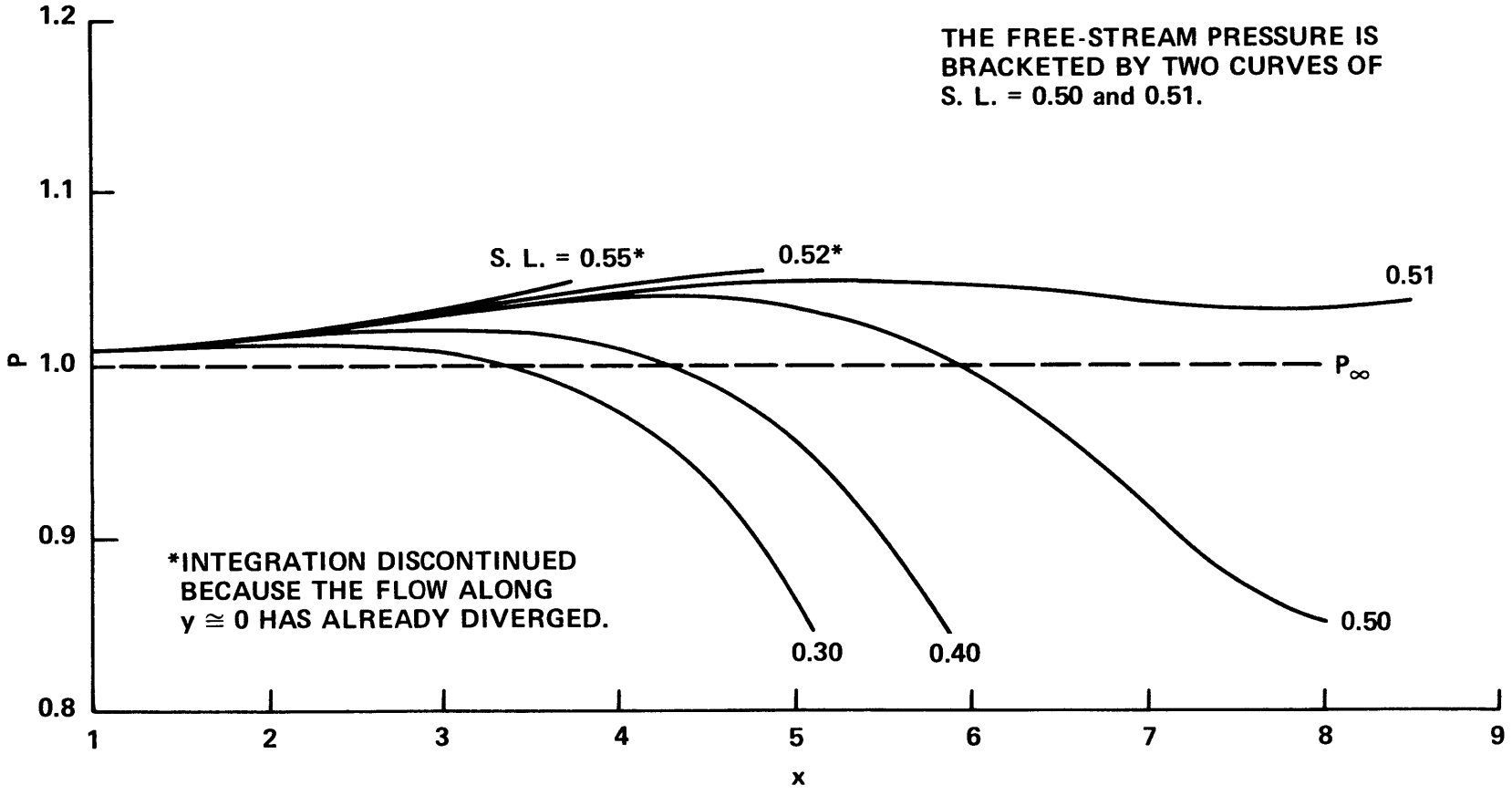

Figure 9b – y ≅ 1.75

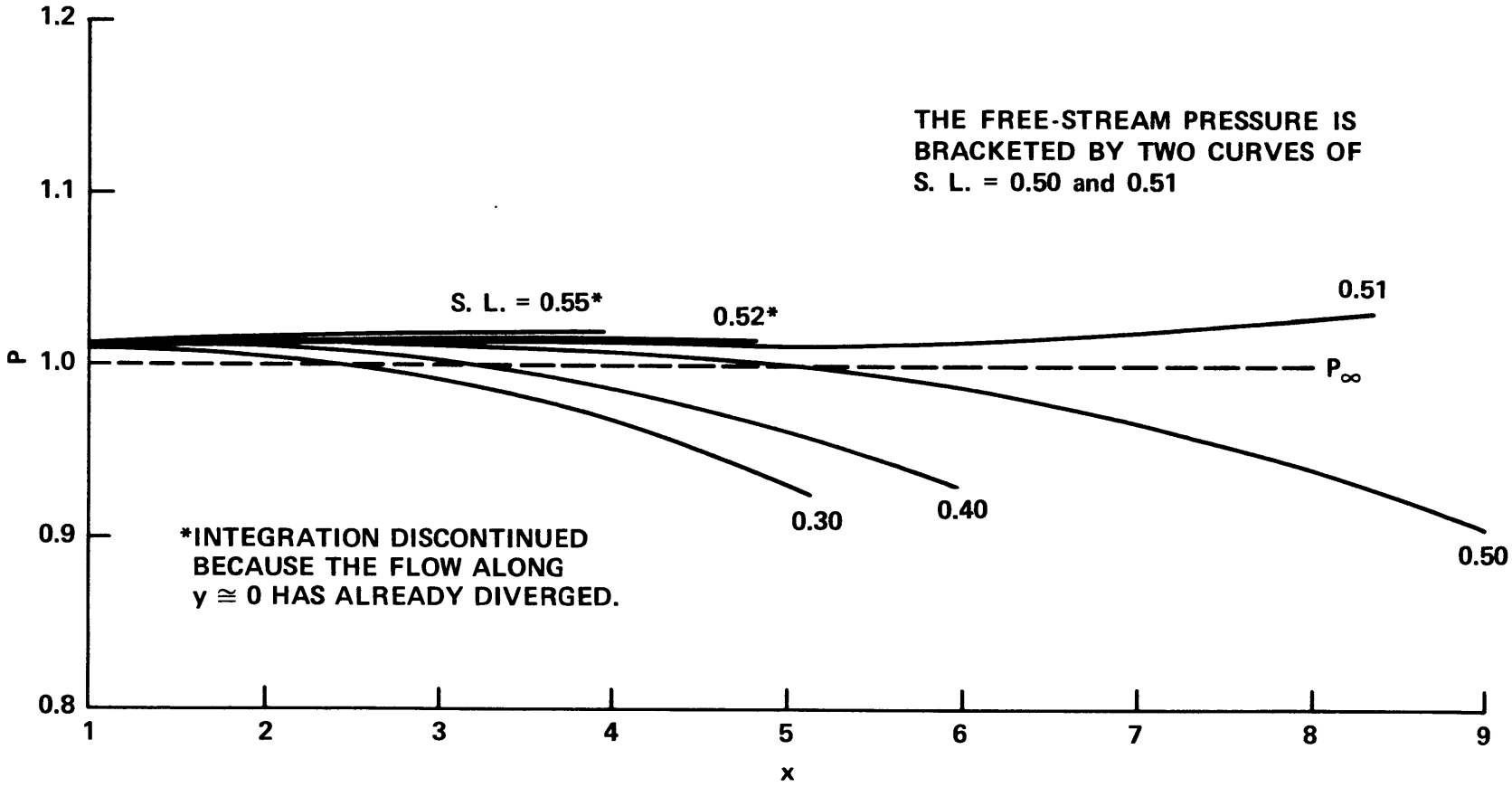

Figure 9c – y ≅ 3.50

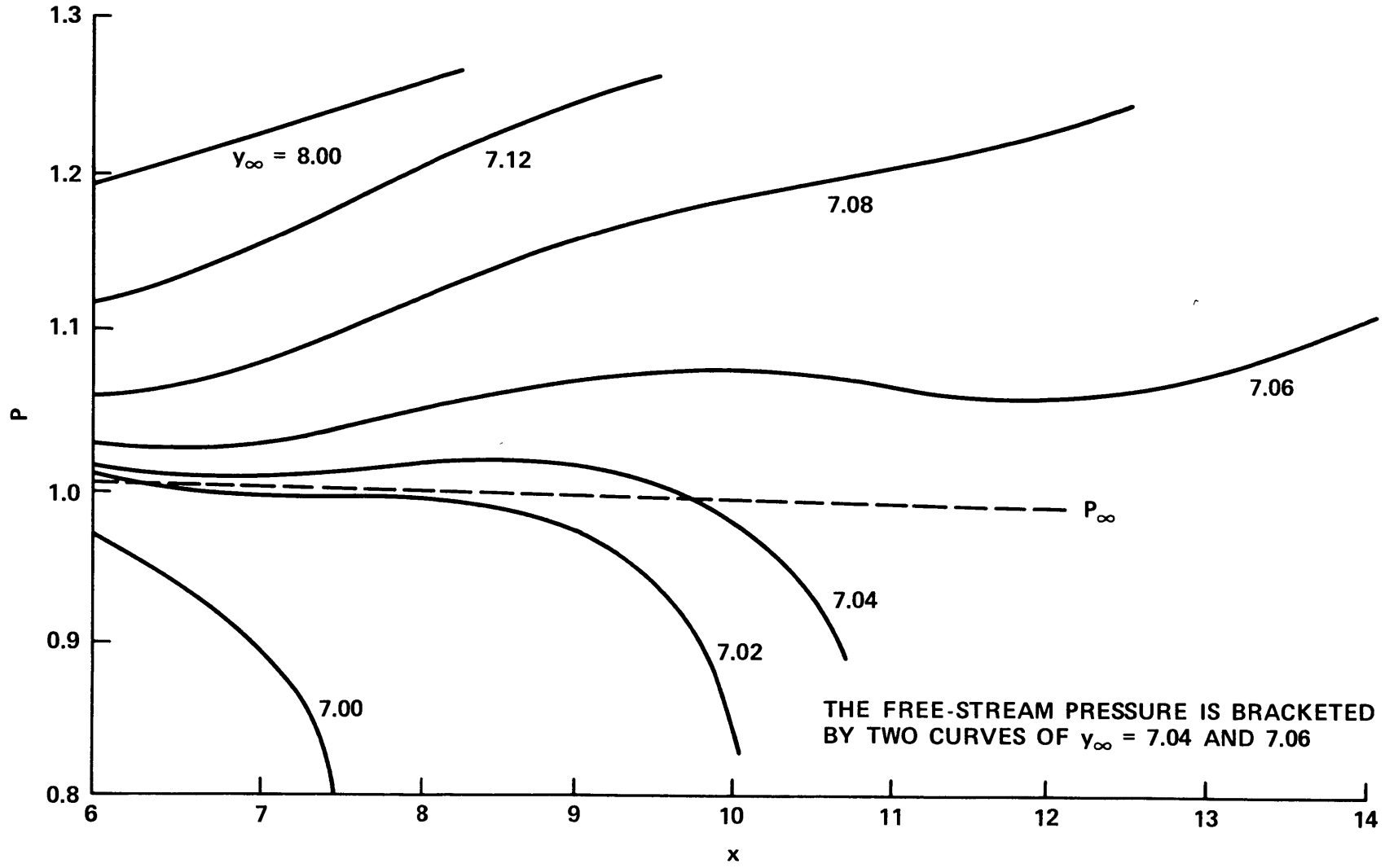

Figure 10a – $y \cong 0$

Figure 10 – Downstream Pressure Distribution in Lower Region for a NACA 0015 Airfoil at M_∞ = 0.729 and α = 4 Degrees

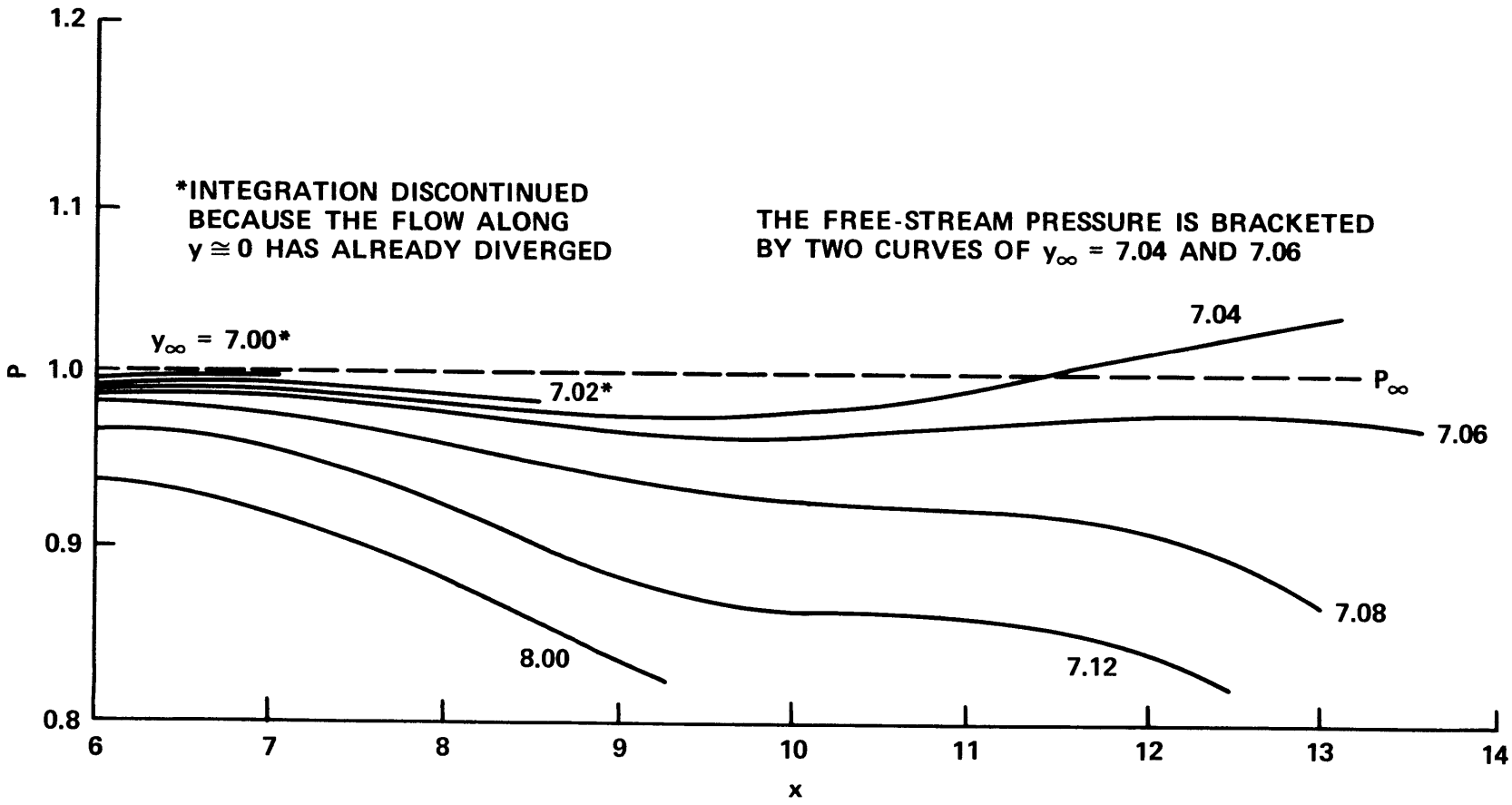

Figure 10b – y ≅ 1.75 to 2.00

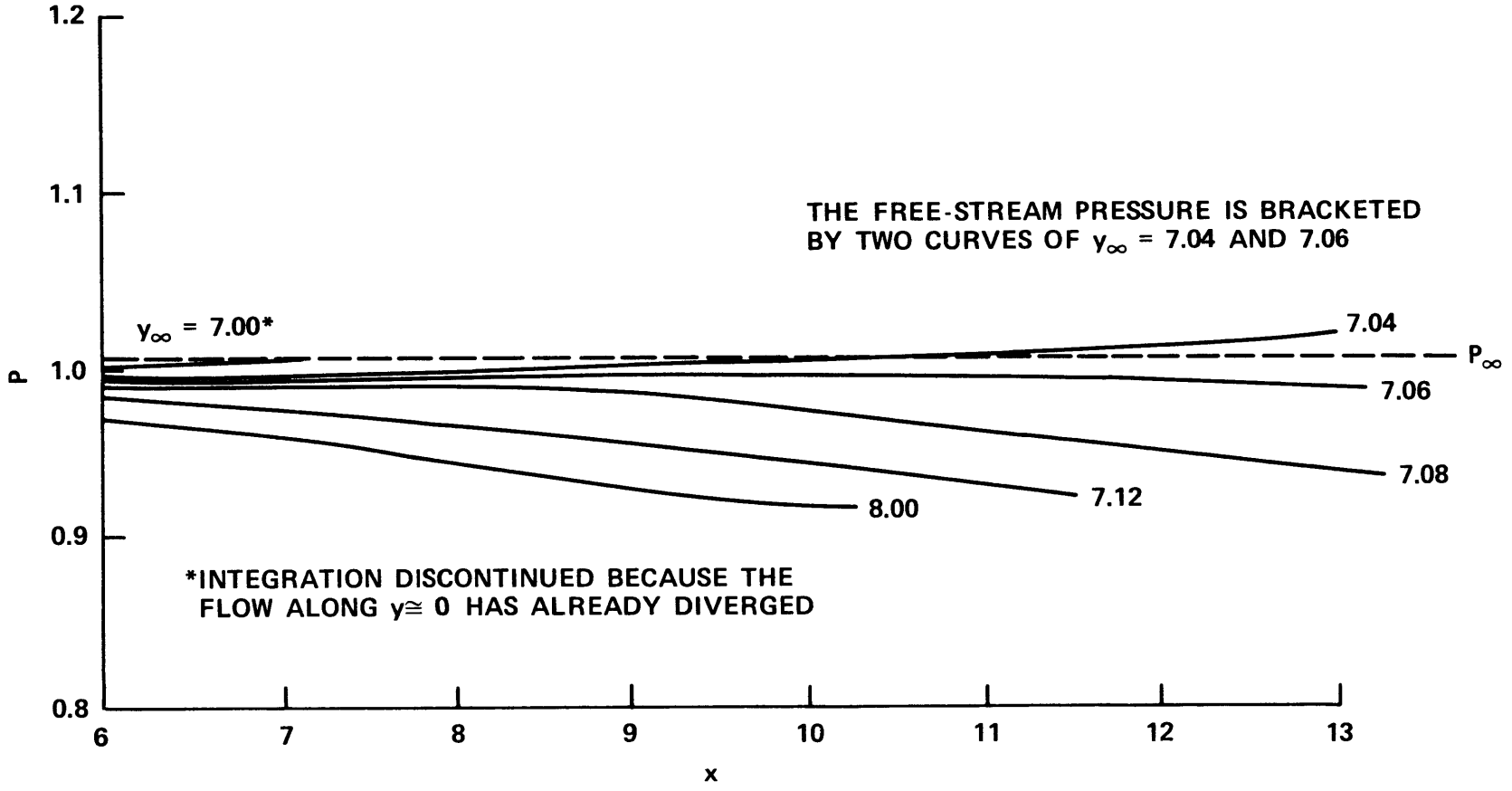

Figure 10c – y≅ 3.50 to 4.00

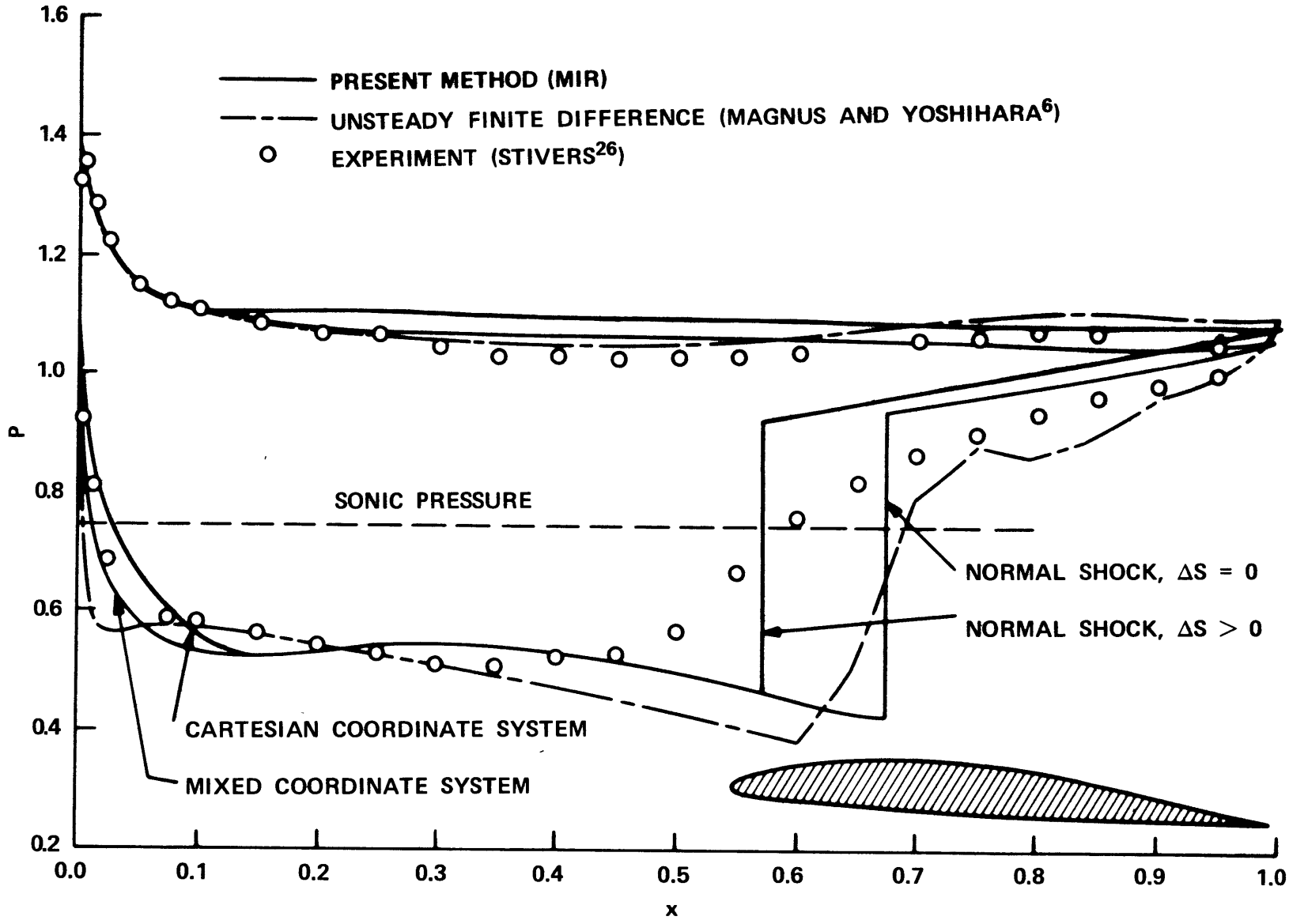

Figure 11 – Pressure Distribution on an NACA 64A410 Airfoil at $M_\infty = 0.72$ and $\alpha = 4$ Degrees

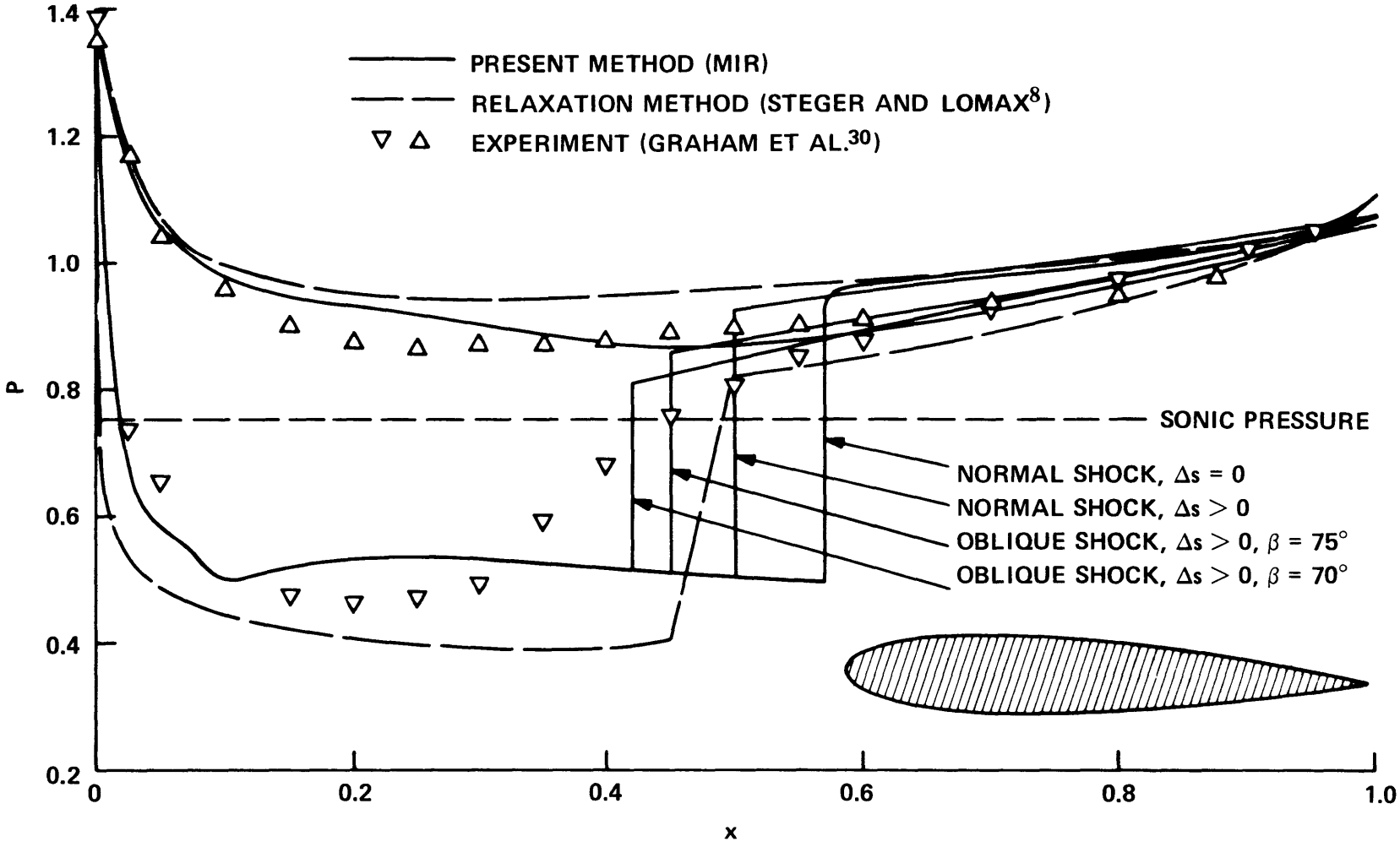

Figure 12 – Pressure Distribution on an NACA 0015 Airfoil at $M_\infty = 0.729$ and $\alpha = 4$ Degrees

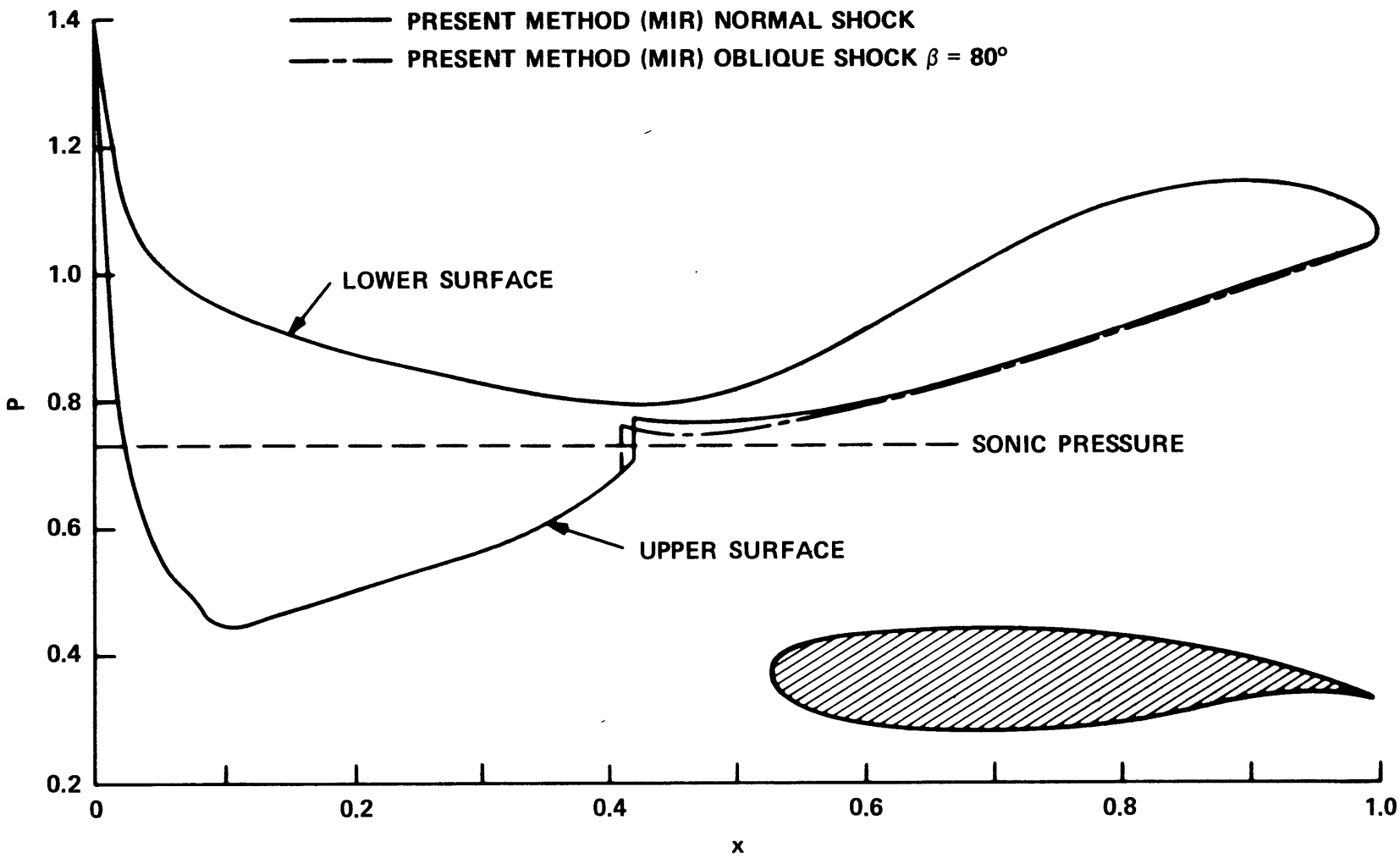

Figure 13 – Pressure Distribution on an Advanced Airfoil at M_∞ = 0.70 and α = 1.5 Degrees

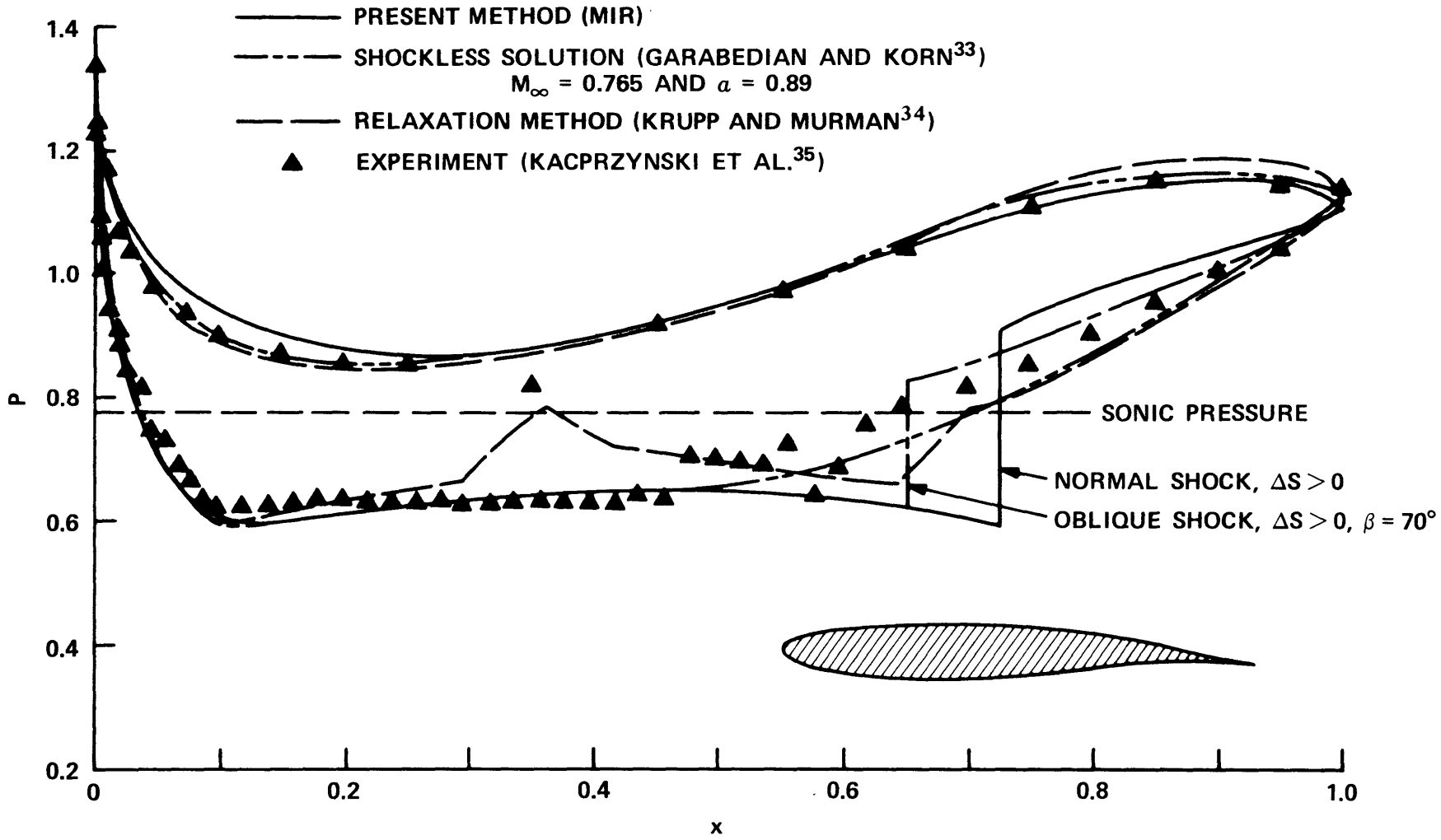

Figure 14 – Pressure Distribution on a Garabedian-Korn Airfoil at $M_\infty = 0.75$

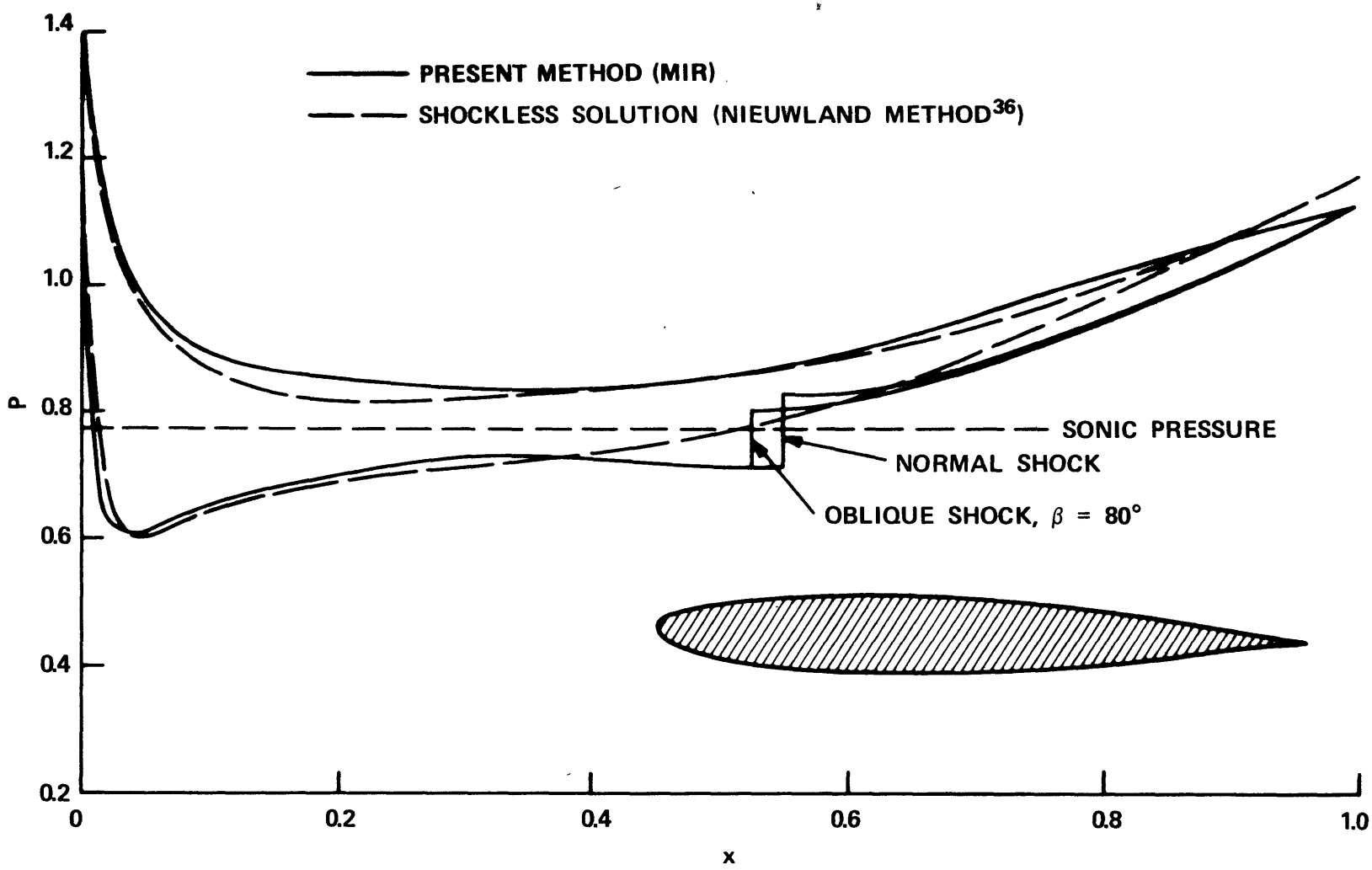

Figure 15 – Pressure Distribution on a Nieuwland Airfoil at $M_\infty = 0.7557$ and $\alpha = 1.32$ Degrees

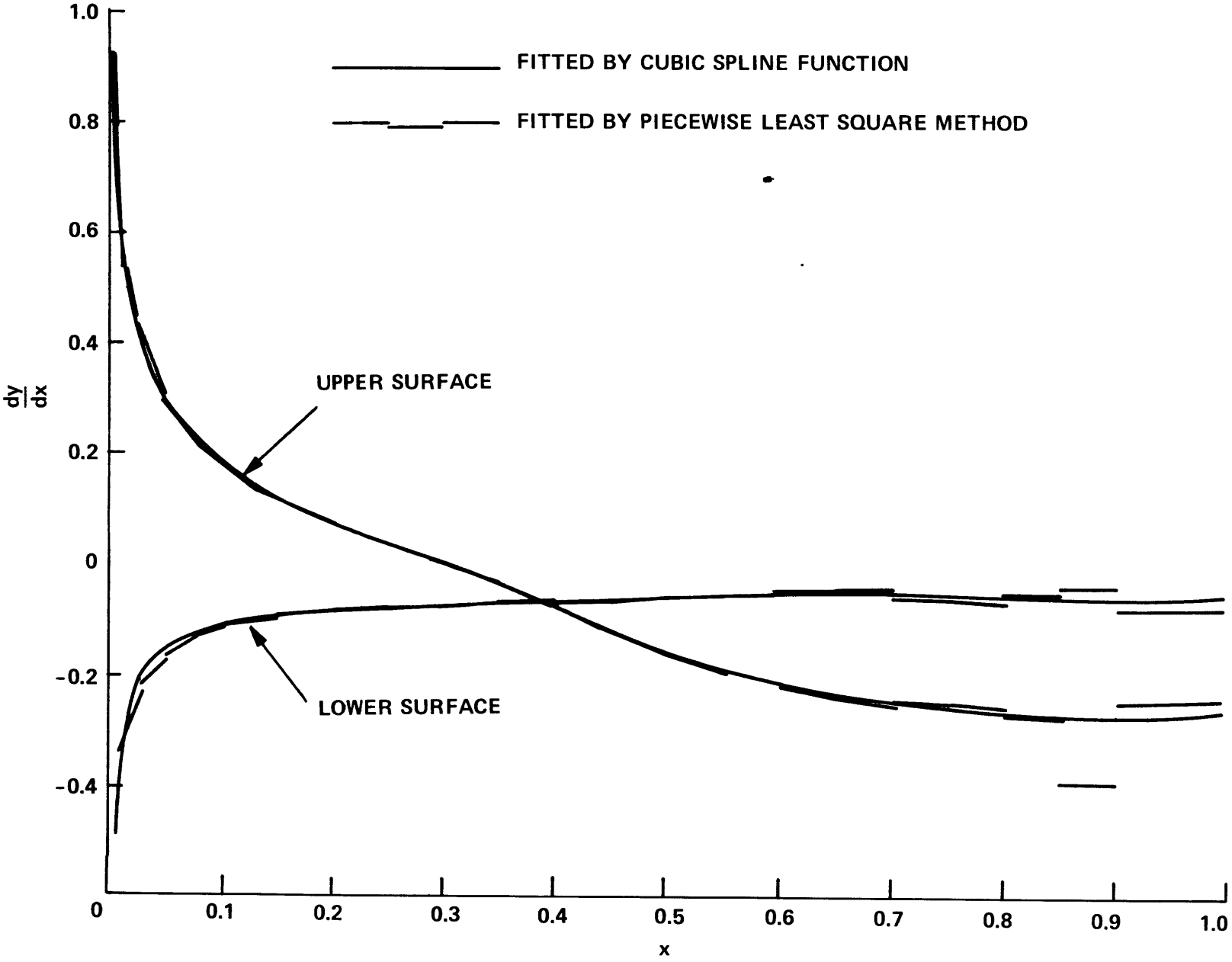

Figure 16 – Slopes of an NACA 64A410 Airfoil at α = 4 Degrees

REFERENCES

1. Tai, T.C., "Application of the Method of Integral Relations to Transonic Airfoil Problems: Part I - Inviscid Supercritical Flow over Symmetric Airfoil at Zero Angle of Attack," NSRDC 3424 (Sep 1970); also presented as Paper 71-98, AIAA 9th Aerospace Sciences Meeting, New York, N.Y. (Jan 1971).

2. Newman, P.A. and D.O. Allison, "An Annotated Bibliography on Transonic Flow Theory," NASA TM X-2363 (Sep 1971).

3. Murman, E.M., "Computational Methods for Inviscid Transonic Flows with Imbedded Shock Waves," Boeing Scientific Research Laboratories Document D1-82-1053 (1971); also presented in AGARD-VKI Lecture Series on Numerical Methods in Fluid Dynamics, Rhode-Saint-Genese, Belgium (Mar 1971).

4. Norstrud, H., "A Review of Transonic Flow Theory," Lockheed-Georgia Company, Report ER-11138(L) (Aug 1971); also presented as Paper at University of Illinois Seminar (Mar 1971).

5. Yoshihara, H., "Some Recent Developments in Planar Inviscid Transonic Airfoil Theory," AGARDograph 156, North Atlantic Treaty Organization (Feb 1972).

6. Magnus, R. and H. Yoshihara," Inviscid Transonic Flow over Airfoils," General Dynamics/Convair Division Report (1969); also presented as Paper 70-47, AIAA 8th Aerospace Sciences Meeting, New York, N.Y. (1970).

7. Murman, E.M. and J.D. Cole, "Calculation of Plane Steady Transonic Flows," AIAA J., Vol. 9, No. 1, (Jan 1971), pp. 121-141 (AIAA Paper No. 70-188, 1970).

8. Steger, J.L. and H. Lomax, "Numerical Calculation of Transonic Flow About Two-Dimensional Airfoils by Relaxation Procedures," presented as AIAA Paper 71-569 at AIAA 4th Fluid and Plasma Dynamics Conference, Palo Alto, California (Jun 1971).

9. Holt, M. and B.S. Masson, "The Calculation of High Subsonic Flow Past Bodies by the Method of Integral Relations," Second International Conference on Numerical Methods in Fluid Dynamics, University of California,

Berkeley (Sep 1970).

10. Melnik, R.E. and D.C. Ives, "Subcritical Flows of Two-Dimensional Airfoils by a Multistrip Method of Integral Relations," Second International Conference on Numerical Methods in Fluid Dynamics, University of California, Berkeley (Sep 1970).

11. Sato, J., "Application of Dorodnitsyn's Technique to Compressible Two-Dimensional Airfoil Theories at Transonic Speeds," National Aerospace Laboratory Technical Report TR-220T (Tokyo, Japan) (Oct 1970).

12. Emmons, H.W., "Flow of a Compressible Fluid past a Symmetrical Airfoil in a Wind Tunnel and Free Air," NASA TN 1746 (Nov 1948).

13. Sichel, M., "Structure of Weak Non-Hugoniot Shocks," Physics of Fluids, Vol. 6, No. 5, pp. 653-662 (May 1963).

14. Ferrari, C. and F.G. Tricomi, "Transonic Aerodynamics," Translated by R.H. Cramer, Academic Press (1968).

15. Sinnot, C.S., "On the Prediction of Mixed Subsonic/Supersonic Pressure Distributions," J. Aerospace Sciences, Vol. 27, pp. 767-778 (1960).

16. Nieuwland, G.Y., "Transonic Potential Flow around a Family of Quasi-Elliptical Aerofoil Sections," National Aerospace Laboratory (Amsterdam) Technical Report T-172 (Jul 1967).

17. Korn, D.G., "Computation of Shock-Free Transonic Flows for Airfoil Design," New York University Courant Institute of Mathematical Sciences, Report NYO-1480-125 (Oct 1969).

18. Boerstoel, J.W. and R. Uijlenhoet, "Lifting Airfoils with Supercritical Shockless Flow," ICAS Paper 70-15, 7th Congress of the International Council of the Aeronautical Sciences, Rome, Italy (Sep 1970).

19. Morawetz, C.S., "The Dirichlet Problem for the Tricomi Equation," Convn. Pure Appl. Math, Vol. 23, pp. 587-601 (Jul 1970).

20. Belotserkovskii, O.M. and P.I. Chushkin, "The Numerical Solution of Problems in Gas Dynamics," in "Basic Developments in Fluid Dynamics," Vol. 1, edited by M. Holt, Academic Press (1965).

21. Chushkin, P.I., "Subsonic Flow of a Gas past Ellipses and Ellipsoids," Translation of Vychislitel'naya Maternatika (USSR), No. 2, pp. 20-44 (1957).

22. Chushkin, P.I., "Computation of Supersonic Flow of Gas past Arbitrary Profiles and Bodies of Revolution (The Symmetric Case)," Translation of Vychislitel'naya Maternatika (USSR), No. 3, pp. 99-110 (1958).

23. Tai, T.C., "Streamline Geometry and Equivalent Radius over a Flat Delta Wing with Cylindrical Leading Edge at an Angle of Attack," NSRDC Report 3675 (Oct 1971).

24. Ahlberg, J.H. et al., "The Theory of Splines and Their Applications," Academic Press (1967).

25. Klineberg, J.M., et al., "Theory of Exhaust-Plume/Boundary-Layer Interactions at Supersonic Speeds," AIAA J., Vol. 10, No. 5, pp. 581-588 (May 1972).

26. Stivers, L.S., Jr., "Effects of Subsonic Mach Numbers of the Forces and Pressure Distributions on Four NACA 64A-Series Airfoil Section at Angles of Attack as High as 28°," NACA TN 3163 (Mar 1954).

27. Liepmann, H.W. and A. Roshko, "Elements of Gas Dynamics," Wiley, N.Y. (1957).

28. Hayes, W.D., "Pseudotransonic Similitude and First Order Wave Structure," J. Aero. Sci., Vol. 21, No. 11, pp. 721-730 (Nov 1954).

29. Pan, Y.S. and M.O. Varner, "Studies on Sonic Boom at High Mach Numbers," AIAA Paper No. 72-652, presented at AIAA 5th Fluid and Plasma Dynamics Conference, Boston (June 1972).

30. Graham, D.J., et al., "A Systematic Investigation of Pressure Distribution at High Speeds over Five Representative NACA Low-Drag and Conventional Airfoil Sections," NACA Report 832 (1945).

31. Spreiter, J.R. and A.Y. Alksne, "Thin Airfoil Theory Based on Approximate Solution of the Transonic Flow Equation," NACA Report 1359 (1958), Supersedes NACA TN 3970.

32. Pearcey, H.H., "The Aerodynamic Design of Section Shapes for Swept Wings," in "Advances in Aeronautical Sciences," Pergamon Press, Inc., Vol. 3, pp. 277-322 (1961).

33. Garabedian, P.R. and D.G. Korn, "Numerical Design of Transonic Airfoils," in "Numerical Solution of Partial Differential Equations," Academic Press, N.Y., Vol. 2, pp. 253-271 (1971).

34. Krupp, J.A. and E.M. Murman, "The Numerical Calculation of Steady Transonic Flows Past Thin Lifting Airfoils and Slender Bodies," AIAA Paper 71-566 (1971), see also Boeing Scientific Research Laboratories Report D180-12958-1 (Jun 1971).

35. Kacprzynski, J.J. et al., "Analysis of the Flow past a Shockless Lifting Airfoil in Design and Off-Design Conditions," Nat'l. Res. Council of Canada (Ottawa) Aero Report LR-554 (Nov 1971).

36. Lock, R.C., "Test Cases for Numerical Methods in Two-Dimensional Transonic Flows," AGARD Report 575 (Nov 1970).

INITIAL DISTRIBUTION

Copies

1 Chief of R&D (ABMDA)

1 U.S. Army Missile Command

3 CHONR
- 1 430B
- 1 432
- 1 461

1 USNA

1 USNPGSCOL

12 NAVAIRSYSCOM
- 1 AIR 03A
- 1 AIR 03C
- 1 AIR 310
- 3 AIR 320
- 1 AIR 5108
- 4 AIR 5301
- 2 AIR 604

2 NAVORDSYSCOM

1 NADC

1 NWC

4 NOL
- 1 Dept. of Aerodynamics
- 1 Dr. K.Y. Chien
- 1 Dr. A.H. Van Tuyl
- 1 Dr. T.F. Zien

1 NWL

1 NATC

1 NAVMISCEN

1 AFOSR

1 OAR, Holloman AFB

1 AF Inst of Technology

1 AEDC

12 DDC

Copies

10 NASA
- 3 HQ, Washington, D.C.
- 4 Ames Research Center
  - 1 Library
  - 1 Dr. J.M. Klineberg
  - 1 Dr. E. Murman
  - 1 Dr. J.L. Steger
- 2 Langley Research Center
  - 1 Library
  - 1 Mr. P.A. Newman
- 1 Lewis Research Center

2 National Science Foundation

1 Polytechnic Institute of Brooklyn
Graduate Center Library
Long Island, N.Y. 11735

1 Brown University
Division of Engineering
Providence, Rhode Island 02912

1 California Institute of Technology
Pasadena, California 91109
Attn: Graduate Aeronautical Labs.
Aero. Librarian

1 University of California
Berkeley, California 94720
Attn: Dr. M. Holt, Div. of
Aeronautical Sciences

1 University of California
Los Angeles, California 90024
Attn: Dr. J.D. Cole
School of Engr. and Applied
Sciences

1 University of California
La Jolla, California 92037
Dept. of Aero. and Mechanical
Engineering Sciences

1 University of Southern California
Los Angeles, California 90007
Attn: Dept. of Aerospace Engr.

Copies

1 Catholic University of America
Washington, D.C. 20017

1 University of Cincinnati
Cincinnati, Ohio 45221
Attn: Dept. of Aerospace Engineering

2 Clemson University
Clemson, S.C.
1 Dr. T. Yang, Dept. of Mech. Engineering
1 Library

1 Cornell University
Ithaca, N.Y. 14850
Attn: Graduate School of Aero Engineering

1 Georgia Institute of Technology
Atlanta, Georgia 30332
Attn: Dr. Ben T. Zinn
Aerospace Engr. Dept.

1 Harvard University
Cambridge, Massachusetts 02138
Attn: Gordon McKay Library

1 Johns Hopkins University
Baltimore, Maryland 21218

1 University of Illinois
Urbana, Illinois 61801
Attn: Aeronautical and Astronautical Engr. Dept.

2 University of Maryland
College Park, Maryland 20740
Attn: Dr. S.I. Pai, Institute for Fluid Dynamics and Applied Mathematics
Attn: Library

1 Massachusetts Institute of Tech.
Cambridge, Massachusetts 02139

1 University of Michigan
Ann Arbor, Michigan 48104
Attn: Library

1 New York University
University Heights
New York, N.Y. 10453

Copies

2 New York University
Courant Institute of Math. Sciences
New York, N.Y.
Attn: Dr. P.R. Garabedian
Attn: Dr. D.G. Korn

2 University of North Carolina
Chapel Hill, N.C. 27514
Attn: Dept. of Aero. Engineering
Attn: Library

2 North Carolina State University
Raleigh, N.C. 27607
Attn: Dr. F.R. DeJarnette
Dept. of Mechanical and Aerospace Engineering
Attn: Library

1 Ohio State University
Columbus, Ohio 43210

1 Pennsylvania State University
University Park, Penn. 16802
Attn: Dept. of Aerospace Engr.

1 Princeton University
Princeton, N.J. 08540
Attn: Dept. of Aerospace and Mechanical Sciences

1 Purdue University
Lafayette, Indiana 47907
Attn: Dept. of Aeronautical Engr. and Astronautics

1 Stanford University
Stanford, California 94305
Attn: Dr. J.R. Spreiter
Dept. of Applied Mechanics and Aeronautics and Astronautics

2 University of Tennessee Space Institute
Tullahoma, Tenn. 37388
Attn: Dr. Y.S. Pan
Attn: Dr. J.M. Wu

2 University of Virginia
Charlottesville, Virginia 22901
Attn: Alderman Library
Attn: Dept. of Aerospace Engr.

Copies

2 Virginia Polytechnic Institute
Blacksburg, Virginia 24061
Attn: Carol M. Newman Library
Attn: Aerospace Engr. Dept.

1 University of Washington
Seattle, Washington 98105
Attn: Dept. of Aeronautics
and Astronautics

1 West Virginia University
Morgantown, West Virginia 26506
Attn: Dept. of Aerospace Engr.

1 Aerospace Research Laboratories
Dayton, Ohio

1 American Institute of
Aeronautics and Astronautics
New York, N.Y. 10019

2 Boeing Company
Seattle, Washington 98124
Attn: Dr. R.C. Gunness
Attn: Mr. A.S. Mahal

1 Cornell Aeronautical Lab, Inc.
Buffalo, N.Y.
Attn: Aerodynamics Research
Department

1 General Dynamics Corp.
Fort Worth, Texas 76101
Attn: Dr. F.K. Enseki

1 CONVAIR Division of General
Dynamics Corp.
San Diego, California 92112
Attn: Dr. H. Yoshihara

2 Grumman Aerospace Corp.
Long Island, N.Y. 11714
Attn: Dr. D.C. Ives
Attn: Dr. R.E. Melnik

1 Institute for Defense Analyses

1 Lockheed-Georgia Company
Marietta, Georgia
Attn: Dr. H. Norstrud

1 LTV Aerospace Corporation
Vought Aeronautics Division
Dallas, Texas 75222

Copies

1 McDonnell Douglas Corporation
Long Beach, California
Attn: Mr. A.M.O. Smith

1 Nielsen Engineering and Research, Inc.
Mountain View, California

1 North American Rockwell Corporation
Columbus, Ohio 43216

1 Northrop Corporate Labs
Hawthorne, California 90250
Attn: Dr. B.S. Masson

1 TRW Systems Group
Redondo Beach, California 90278
Attn: Dr. D.R.S. Ko

CENTER DISTRIBUTION

25 1670

UNCLASSIFIED
Security Classification

DOCUMENT CONTROL DATA - R & D

(Security classification of title, body of abstract and indexing annotation must be entered when the overall report is classified)

1 ORIGINATING ACTIVITY (Corporate author)	2a. REPORT SECURITY CLASSIFICATION
Aviation and Surface Effects Department Naval Ship Research and Development Center Bethesda, Maryland 20034	Unclassified 2b. GROUP

3 REPORT TITLE

APPLICATION OF THE METHOD OF INTEGRAL RELATIONS (MIR) TO TRANSONIC AIRFOIL PROBLEMS. PART II - INVISCID SUPERCRITICAL FLOW ABOUT LIFTING AIRFOILS WITH EMBEDDED SHOCK WAVE

4 DESCRIPTIVE NOTES *(Type of report and inclusive dates)*

Research and Development Report

5. AUTHOR(S) *(First name, middle initial, last name)*

Tsze C. Tai

6 REPORT DATE	7a. TOTAL NO. OF PAGES	7b. NO. OF REFS
July 1972	71	36

8a. CONTRACT OR GRANT NO	9a. ORIGINATOR'S REPORT NUMBER(S)
NAVAIR TASK R230.201 b. PROJECT NO. c. NSRDC 1670-277 d.	NSRDC Report 3424 Part II 9b. OTHER REPORT NO(S) *(Any other numbers that may be assigned this report)* Aero Report 1176

10. DISTRIBUTION STATEMENT

Approved for public release; distribution unlimited

11 SUPPLEMENTARY NOTES	12. SPONSORING MILITARY ACTIVITY
	Commander Naval Air Systems Command (AIR-320) Washington, D. C. 20360

13 ABSTRACT

Numerical procedures developed in Part I of the present report for applying the method of integral relations to transonic airfoil problems are extended here to lifting cases. A modification of the strip arrangement described in Part I now enables any desired number of strips and size of integration domain to be used. The full inviscid flow equations (may be rotational) are employed and approximated by second-order polynomials in transverse direction in a physical plane. Numerical procedures including iterative processes for solving subject two-point boundary value problems are formulated for the case of high subsonic free-stream Mach numbers. Cartesian coordinates are employed except near the leading edge region where the use of a body coordinate system is convenient to account properly for large slope variation there. The geometry of the airfoil is represented by cubic spline functions when a closed airfoil relation is not available. The effect of change of entropy across the embedded shock wave is examined by allowing a decrease in total pressure after the shock wave along the surface streamline. With the shock angle as a free parameter, oblique shock relations as well as normal shock relations can be incorporated in the solution.

Results are presented for supercritical flows past various airfoils, including two conventional, one advanced, and two shockless airfoils. Comparisons of the results with existing theoretical and/or experimental data indicate reasonably good agreements. It is found that the shock location moves forward in the case of a finite increase in entropy across the shock wave; the entropy has, therefore, a cumulative effect on the flow.

14 KEY WORDS	LINK A		LINK B		LINK C	
	ROLE	WT	ROLE	WT	ROLE	WT
Integral Relations						
Lifting Airfoils						
Inviscid Flows						
Supercritical Flow						
Subcritical Flow						
Nonisentropic Flow						
Normal Shock						
Oblique Shock						
Spline Function						